

Analytical Methods

Accepted Manuscript



This is an *Accepted Manuscript*, which has been through the Royal Society of Chemistry peer review process and has been accepted for publication.

Accepted Manuscripts are published online shortly after acceptance, before technical editing, formatting and proof reading. Using this free service, authors can make their results available to the community, in citable form, before we publish the edited article. We will replace this *Accepted Manuscript* with the edited and formatted *Advance Article* as soon as it is available.

You can find more information about *Accepted Manuscripts* in the [Information for Authors](#).

Please note that technical editing may introduce minor changes to the text and/or graphics, which may alter content. The journal's standard [Terms & Conditions](#) and the [Ethical guidelines](#) still apply. In no event shall the Royal Society of Chemistry be held responsible for any errors or omissions in this *Accepted Manuscript* or any consequences arising from the use of any information it contains.

ARTICLE

Microelemental characterisation of Aboriginal Australian natural Fe oxide pigments

Cite this: DOI: 10.1039/x0xx00000x

R. S. Popelka-Filcoff,^a C. E. Lenehan,^a E. Lombi,^b E. Donner,^b D. L. Howard,^c M. D. de Jonge,^c D. Paterson,^c K. Walshe,^d A. Pring^{a,d}

Received 00th January 2012,
Accepted 00th January 2012

DOI: 10.1039/x0xx00000x

www.rsc.org/

This manuscript presents the first comprehensive microcharacterisation of Fe oxide minerals used in Aboriginal Australian mineral pigments. The combination of X-ray fluorescence microscopy (XFM) and light microscopy provides a broad characterisation as well as the ability to spatially match visual observation with elemental composition. A novel method for casting pigment samples in a pattern on a slide was used for consistent elemental mapping. Semiquantitative bulk data was also collected and compared to the microscopic and microelemental data. These analyses demonstrate the ability to document the variability in ochre pigments in Australia, as well as which elements drive the variation within and between ochre source locations. The methods developed provide a more comprehensive understanding of other complex natural mineral pigments worldwide.

Introduction

Ochre and related natural Fe oxide pigments are a significant material in Indigenous cultures worldwide. Ochre pigments are utilised for their durability and widespread availability as observed in rock art from thousands of years ago, as well as their cultural symbolism in colour in modern times. In Aboriginal Australia, Fe-based mineral pigments are found in nearly every cultural context from a diverse array of cultural objects (shields, spears, boomerangs, bark paintings and others), in archaeological remains and rock art. Ochre continues to have strong cultural traditions in the present day. Examples of this include the use of natural mineral pigments in contemporary art centres such as those in the Kimberley region of Western Australia, and the use of ochre pigments on the body.^{1,2}

To visual inspection (approximately 10 cm distance) natural ochre pigments can appear to be homogeneous with a solid coverage of the substrate at a uniform thickness and particle size and shape. However under magnification, it can be observed that the pigments are composed of a range of particle shapes and sizes, and in many cases a range of colours. This distribution of natural pigmented particles, often caused by accessory minerals has not been well characterised.

In addition, the pigments adhere to the substrate with a degree of variation depending on the method of application, type of

substrate, type of binder and any variability in the substrate itself. Variation in these factors include whether the pigment is applied by hand or by brush or other implement. Typical substrates for Aboriginal Australian objects include bark, wood and plant fibres, or in the case of rock art, natural rock substrates. Various types of binders were also used for mixing pigments, which include water and various plant and animal materials.^{3,4}

Ochre is a complex mixture of Fe oxides and other minerals that can include calcite, gypsum, clays and feldspars. Iron oxides occur in varied geological formations, including red beds, banded iron formations, gossans and sediments. Ochre formations are also prevalent in soils that can contain several Fe-oxide minerals simultaneously.⁵ Each ochre carries a chemical and mineralogical “signature” that reflect the diagenetic processes of the source. Sampling across a deposit provides information on the local variability of the geochemical signature. It has been demonstrated that a single sample from a site is not necessarily characteristic of a single geochemical composition of the site, due to geological variability within the mine or quarry.^{6,7} Characterisation of multiple samples from within a site is essential to give a more complete assessment of the diversity within the site. For these samples, neutron activation analysis (NAA) provides elemental data on variability between bulk samples on the order of 50-100 mg as single concentration values for 30+ elements per sample. Previous studies have demonstrated that NAA data used with

1 multivariate statistical techniques can characterise individual
2 sources geochemistry on the bulk scale as well as differentiate
3 ochre sites from each other. While these data are valuable for
4 understanding the source geochemical variability on a large
5 scale, the variability at the micron scale of the ochre cannot be
6 determined by NAA. The Fe oxides in ochre are known to be
7 admixed with a range of accessory minerals such as clays,
8 calcites and others, however the contribution of each mineral to
9 the characteristic geochemical signatures is unknown.⁸
10 Therefore an elemental examination of the ochre on the micron
11 level is essential to understand not only the elemental
12 composition of the ochre material and minerals, but also the
13 inherent variability of micron-sized particles of minerals that
14 compose the complex ochre mixture. An analysis of this scale
15 provides not only information on the elemental distribution of
16 the sample, but also spatial and morphological information on
17 the elemental distributions. While recent advances in scanning
18 electron microscopy (SEM) coupled with elemental analysis
19 (EDAX), have allowed elemental raster mapping of samples,
20 the resolution is generally on the order of 100 microns. In
21 addition, the maps produced are low resolution and not
22 representative of the fine structure of the surface. Samples
23 introduced to the SEM are limited to those that are small
24 enough (< 2mm diameter stub) to fit into the chamber and that
25 can tolerate high vacuum conditions, and potentially coated
26 with carbon or gold for imaging purposes. None of the above
27 conditions are acceptable for artefacts or ochre from cultural
28 heritage materials.

31 X-ray fluorescence microscopy (XFM) as a form of micro-XRF
32 analysis performed at the Australian Synchrotron (AS) provides
33 the necessary analysis on the elemental level to understand the
34 original source variability of complex natural mineral ochre
35 pigments. Using the Maia detector provides high resolution
36 mapping of individual particles inherent in the original sourced
37 or archaeological ochre sample. In addition, unlike NAA, XFM
38 requires only micrograms of material and is non destructive.
39 XFM can analyse larger areas (on the order of cm) on many
40 sample types with much higher sensitivity than SEM- EDAX.
41 These capabilities are ideal for cases where trace elements can
42 be diagnostic in terms of fingerprinting and where these trace
43 elemental distributions may be smaller than SEM resolution of
44 100 micron or where the presence of the element was unknown.
45 XFM can further be used to analyse cultural heritage artefacts
46 as well as individual pigment samples, which is not possible
47 using SEM-EDAX or NAA. A comparison of the individual
48 pigment samples to the artefact provides a valuable advantage
49 of a direct data comparison and technique from sample to
50 artifact. A few prior studies have demonstrated successful
51 application of XFM to cultural pigments.⁹⁻¹³

52
53
54 Recently there have been several studies that have explored a
55 range of techniques with the aim of developing methods for
56 establishing the provenance of ochre and pigments with
57 archaeological and ethnographic associations including possible
58 trade routes.^{1, 6, 7, 14-16} However, many of these studies are

based on the analysis of the bulk of the material, with such
techniques as neutron activation analysis (NAA) and laser
ablation inductively coupled plasma mass spectrometry (LA-
ICP-MS).^{6, 7, 17} However there is one recent study on the
characterisation of Australian ochre using synchrotron XRD
and PIXE.¹⁸ There are a few studies utilising microscopy of Fe
oxides, however these concern the mineral properties and not
the cultural aspects.⁵

This manuscript will focus on the multiple samples taken from
five well known and documented ochre sources from Australia:
Bookartoo (also spelled Bukartu and Pukatoo) (South
Australia), Karrku (Northern Territory), Moana (South
Australia), Pine Point (South Australia) and Wilgie Mia
(Western Australia). Samples from these sites have been
collected over several years by researchers including M. Nobbs,
P. Jones, M. Smith and others associated with the South
Australian Museum and the Western Australian Museum.^{6, 19-26}

Here we describe the first systematic microanalysis and
documentation of ochre samples towards a more complete
understanding and micro-characterisation of Aboriginal
Australian ochre pigments. These data provide a foundation
data set for feasibility studies for the in-beam analysis of
Aboriginal Australian objects from several of the most
significant ochre quarries in Australia and enhances knowledge
of this inherently complex material. This study also expands the
capability of the method towards understanding complex
geological systems and formations, which may also inform
environmental influence on Fe-oxide deposits.

Experimental

Sample Selection

A suite of ochre samples has been assembled from individual
researchers as well as from the South Australian Museum
Archaeology and Ethnographic collections.^{6, 19-26} The majority
of these samples have also been analysed by complementary
techniques such as NAA.^{6, 24} From this larger combined
collection, 165 samples were chosen for analysis by X-ray
fluorescence microscopy (XFM). These 165 samples
represented source (site) samples as well as samples from
archaeological context. Sources in this project are defined as
the original “quarry” or geological formation of the ochre
material; therefore these samples were collected directly from
the source in the field or presumed to be. On the other hand,
archaeological samples may or may not be from the original
quarry as they may have been exchanged through cultural
networks.

Located in the Flinders Ranges, South Australia, Bookartoo
samples have been collected from this extensive site over
different time periods and therefore likely different locations
within the site.^{16, 23, 27} OCH050 and OCH24 were collected by
Margaret Nobbs, whereas the OCH075-76-79A and OCH255

series are from Mike Smith. Karrku, located in the Northern Territory, is the local name for “ochre”.²⁸ The samples were collected by Mike Smith and Barry Fankhauser as part of ochre characterisation studies completed in the 1990s. These samples were collected over a period of two years from the site. Moana is an exposed coastal site near Adelaide (South Australia) and therefore is subject to more intense weathering and effects of the ocean. Geologically, it is a sedimentary site as opposed to Karrku and Bookartoo, which are weathered banded iron formations. Similarly to Moana, Pine Point is an exposed and therefore weathered site on the coast of Yorke Peninsula (South Australia). Wilgie Mia (Western Australia), also a weathered banded iron formation is perhaps the best-known site due to the quality of the ochre and the large scale of the site.²⁹

Sample Preparation

In order to minimise the variation in the original state of the material, a consistent method was implemented to standardise the preparation of the ochre minerals for microscopy and XFM analysis.

All samples were hand ground in a Brazilian agate mortar and pestle to a consistent particle size powder. Samples were dried overnight in a 100° C oven and stored in glass vials. All samples were sieved to < 250 micron using individually cut disposable plastic mesh screens to minimise cross contamination between samples. This step was performed to remove potentially large particles as well as organic material such as grasses and plant fibres. Additionally, the particle size of 250 micron was chosen as a likely maximum size for the use of Indigenous pigments on objects. However, depending on the origins of the pigment and the particular characteristics of the mineral, a variation in particle size and distribution is expected.

A standard microscopy quartz slide (2 x 1 inches, 5.08 x 2.54 cm) was prepared by sanding it with fine grit sandpaper to aid in the attachment of the epoxy cast mineral to the slide. A grid was laid out on the slide with space for 45 samples per slide, in 15 columns and 3 rows (Figure 1). The samples were cast individually in epoxy on a quartz slide in even distribution for ease of analysis by XFM. Duplicates of each slide were also made.

Figure 1: A demonstration slide displaying the sticker mask (light blue, right), with ochre squares cast in resin remaining on the slide after sticker removal (left)

A grid mask was designed to affix to the slide to aid the casting of the samples, to maintain the pattern of 2 x 2 mm squares for each individual sample, separated by 0.5 mm. The grid mask was designed by CAD design and produced in a polymer mask “sticker”. The individual blocks were cut by a blade and removed individually, and each individual sticker was applied to the front face of each slide.

In order to affix the samples permanently to the slides, approximately 5-10 milligrams of each sample were mixed individually with Petropoxy 154 epoxy (Burnham Petrographics) in a glass vial with a glass stirrer in a 50/50 volume. This epoxy was chosen for its known capabilities in mineral slide preparation, fast set time as well as its relatively contaminant-free substrate that would not introduce further elemental impurities. After allowing the epoxy to cure for approximately 60 minutes in an 80° C oven, the samples were applied manually, with the aid of a binocular microscope to each individual well, filling each well with a layer of sample. After the first applications had solidified a second layer for individual samples was applied to each well. After a complete curing of the epoxy to hardness in an 80° C oven for 30 min, the entire slide was allowed to cool and the epoxy to set for several hours until completely cured. The “sticker” mask was then removed with a blade. The entire slide was then cured on a 130° C hotplate for a few minutes. The slides were then polished to approximately 80-100 micron thickness to achieve a consistent thickness of epoxy samples. Figure 2 is an example of one completed slide set with 45 ochre samples. It is expected that the samples will be heterogeneous across the individual sampling squares, but this sampling method will be more representative of a cultural application of a natural ochre pigment to an object. Although there is slight variation in the shape and coverage of each sample, the area in the centre of the square is representative of each sample.

Figure 2: An example of completed slide with the 45 individual ochre samples cast in Petropoxy resin. Each square is approximately 2 mm square, with 0.5 mm between the squares.

XFM beam line parameters

The experiment utilised the standard set up of the XFM experimental parameters with the Maia detector (a 384-element array of 1 x 1 mm Si detectors, oriented axially in backscatter geometry, which is 180° to beam).^{11, 30} X-ray focusing was achieved with Kirkpatrick-Baez mirrors, which provide longer working distance and high sensitivity requirements as compared to other X-ray analysis setups.³⁰ The Australian Synchrotron operated at 3GeV with a stored current of 150-200 mA. During these experiments, the XFM beam had an incident energy of 18.5 keV and a flux of approximately 8×10^8 photons per second.

For the experimental set-up, the individual polished slides were attached to the plexiglass sample holder frame used for XFM measurements. This setup is regularly used for the experiments and also allows for a set distance from the slides to the beam and detector.

Since the area of each slide is relatively small, a smaller step size was chosen to maximise the characterisation of the sub-micron areas of pigment. During the experiments the beam size was 2 micron. The samples were analysed at a rate of 0.768

mm per second with a step size of 2 microns. A sampling area of approximately 0.7 mm high strip through the centre of each row of the samples was chosen for a consistent measurement area of each row and to minimise variation. An area of 36.9 x 0.7 mm was analysed for each row of the slides, producing a total of 11 rows of 15 samples (165 samples total). The slides were analyzed in three separate experiments, but with similar conditions. Data analysis was accomplished using the GeoPIXE software package.^{11, 30}

The elements measured in this study included As, Ca, Cr, Cu, Fe, Ga, Mn, Pb (L line), Rb, Sc, Se, Sr, Ti, V, and Zn. For each pixel, the full XRF spectrum is collected. GeoPIXE is used to deconvolute these individual spectra into elemental concentration maps. Relative concentrations of each element or combinations of elements are indicated by colour and intensity of the colour. For each point in the image as well as for areas in the image, GeoPIXE can determine semiquantitative values of the elements analysed. A rectangular area of 1.664 mm wide x 0.608 mm high was used to calculate the semiquantitative areas and limits of detection for each element for each pigment square. Semiquantitative data were used to compare pigments to each other as well as to compositional data from other techniques.

Light Microscopy

The slides used for XFM analyses were also studied in the light microscopy analysis to provide a direct comparison between the elemental maps and microscopy images. The slides were viewed through an Olympus CX41 transmitted light microscope at 100x. Digital images were captured using an Olympus DP21 camera.

Results and Discussion

XFM Images

Images from the XFM analysis demonstrated the inherent variability of the ochre samples across sources and between sources. While 165 samples were analysed, individual examples from each highlighted site are selected for discussion (Figures 3-6)

Data were acquired for all 15 elements, however, some elements demonstrated very low concentrations and therefore very little data in the maps. These results indicate that the elements in the ochre pigment sample are below detection limits of the technique. Of the elements examined, data for the maps were consistently found for As, Ca, Cr Fe, Mn, Ti, and V. Elemental concentrations for Cu, Ga, Pb, Sc, Se, Sr and Zn were generally close to or below detection limits for the sites highlighted in this study; therefore images are not presented. Prior to this study data for Cu and Pb were unknown for ochre samples, as NAA is not able to analyse for these two elements. These data reveal that Cu and Pb are not diagnostic for identifying or characterising the ochre origin and these

elements will not be discussed further. Table 1 presents the semiquantitative data for the elements analysed and for the sites discussed. The range of values generally agrees with other bulk methods such as NAA within 10-20%.^{6, 7} However there is not a perfect agreement with the bulk methods. NAA is a traceable method that uses certified and reference standards for calculation of values and uncertainties. GeoPIXE utilises a user-supplied model of the specimen matrix, in which the matrix composition (Fe_2O_3), its density (5.24 g cm^{-3}), and uniform thickness ($100 \mu\text{m}$) are used to model the X-ray fluorescence yields. Deviations of the specimen from the assumed matrix parameters will lead to a less accurate determination of sample concentration. The matrix and its thickness will vary between samples, thus we regard the results as semiquantitative. We note that assuming hematite or goethite as a matrix makes negligible difference to the determined concentration, but a grossly different matrix such as silicate will be significant. The sampling size between the two methods is quite different, on the order of mg for XFM as compared to at least 50 mg for NAA, which will influence the samples representation to the bulk. In particular for XFM, the sample is further diluted approximately 1:1 by volume in the epoxy resin, therefore affecting the calculations by GeoPIXE. In general, this will reduce the concentrations by approximately one half for iron and heavier elements, reduce by 30% for V-Cr and increase Ca, Ti by about 30%.

Table 1: Semiquantitative data (in ppm for each element) for each ochre sample as calculated by GeoPIXE, organised by site name. Each area was 1.664 mm wide x 0.608 mm high on each square. Se and Ge and Cu were eliminated from the data set as all values were below detection limits.

Discussion of the elemental maps will follow by element. A further discussion of the sites and their archaeology is discussed elsewhere in the literature.

Figure 3: Microelemental map of Fe for samples from the sites analysed in this study. Images are false coloured to demonstrate relative concentration intensities, with black the lowest and white/yellow the highest. Sites are highlighted in each image.

(a)Bookartoo (b) Karrku (c) Moana (d)Pine Point (e)Wilgie Mia

Fe

As Fe is the main constituent of Fe-oxide ochre pigments, the elemental maps of Fe were studied in more detail to identify trends in the data. Concentrations ranged from 26 ppm to 45%.

BOOKARTOO

Variations can be observed in the overall intensity of the false colour maps but this is likely an effect of the variability in the scaling of the image brightness relative to other samples rather than a reflection of the actual concentration of Fe in each

sample (see below). The samples exhibit a dense coverage of small iron oxide particles with some larger platy iron oxide particles of higher concentration. These data support earlier suggestions of “micaceous” ochre observed from the site.^{19, 23, 27} This ochre is visually a deep purple red, however yellow ochre is also found at this site. OCH079-A is an example of yellow ochre, and its lower Fe concentration indicated is composition of goethite [α -FeO(OH)] rather than hematite (Fe_2O_3), or admixture of yellow iron pigments with other lower-Fe minerals such as siderite (FeCO_3) or jarosite-group minerals ($\text{XFe}_3(\text{SO}_4)_2(\text{OH})_6$ with X = K, Na, Pb etc.

KARRKU

Samples OCH 092-A and OCH 090, OC096 and OCH 094-A display variation in particle size and shape. A plausible reason for this is that the samples were collected during two different campaigns in 1996 and 1998 by Mike Smith et al.; therefore the variation likely reflects different sampling locations. OCH090 and OCH 092 also display more voids as compared to OCH-96-A and OCH094-A, which are more densely covered in Fe concentration. The site is known to contain soft earthy specular hematite between quartzite and is mined in a cave location.²⁶

MOANA

Samples from the sites were obtained from the South Australian Museum, Mike Smith and the Margaret Nobbs collection. OCH020, OCH036, OCH037, OCH019, and OCH278A are from the Nobbs surveys. Remarkably, they demonstrate very low, if any, Fe signal in the elemental maps except for OCH037-A and OCH037-C, which are sub samples from a larger sample. OCH101-A and OCH 101-A were collected by Mike Smith, and demonstrate similar Fe elemental maps to the Nobbs samples. More recent samples OCH283-293 have a similar Fe distribution and profile except OCH 289 However samples 283-293 are similar to OCH-037. Samples OCH 275 and OCH 281 and OCH 254 are also listed as being from Moana, however they are from the Archaeology and Ethnography Collections rather than from a specific researcher survey. Care needs to be taken in the interpretations of these samples as they may not be true source samples, rather examples of ochre collected from an archaeological excavation. Therefore these samples are not representative of the site but perhaps artefact ochre found at the site that had been imported from elsewhere. These samples provide examples as potential “unknowns” for attribution to determined source locations established in this study.

PINE POINT

Similarly to Moana, this site is a coastal weathered site and the relatively low Fe concentrations reflect this. As samples OCH299-309 were sampled directly from the site, they represent the variability within the areas sampled. OCH047 and 048 are from the Nobbs collection and bear more similarity to each other than the other samples, reflecting differing sampling campaigns.

WILGIE MIA

Wilgie Mia and Little Wilgie Mia are both banded iron formations located in Western Australia. A recent paper characterised these materials in the bulk using LA-ICP-MS.¹⁷ The samples from the site again reflect at least three different sampling trips, from Nobbs, Smith and the Western Australian Museum, in order of oldest to most recent. In general the samples are relatively rich in Fe, especially samples such as OCH 117-Y, 260-A and 119, which are composed of high Fe concentration with tightly packed small particles. In contrast OCH 277 and 257, collected by Nobbs, and from the collections of the South Australian Museum, respectively are very low Fe and perhaps not representative of the site.

In general across the five sites discussed, the distribution of the Fe in the samples allows insight into the relationship of the Fe to particular particle sizes and shapes, rather than a bulk analysis. In previous analyses, a distribution in the bulk composition was also observed, with the concentration of Fe ranging from 10-60% iron oxides, depending on the site and mixture.^{6, 7} The large range of Fe composition in the samples as well as several samples having a very low concentration of Fe calls into question the definition of ochre as far as the majority composition of Fe oxides of the material. As ochre is an admixture of Fe-oxides and other minerals, the varying ratios of these materials and types of materials affect the distribution. Elemental analysis cannot provide direct information on the mineralogical state of the material; therefore some Fe-oxides may be hematite or goethite-based.

Figure 4: Microelemental map of Ca for samples from the sites analysed in this study. Images are false coloured to demonstrate relative concentration intensities, with black the lowest and white/yellow the highest. Sites are highlighted in each image. (a)Bookartoo (b) Karrku (c) Moana (d)Pine Point (e)Wilgie Mia

Ca

Ca was an element of interest as at least one site (Bookartoo), the ochre material is found within a dolomite [$\text{CaMg}(\text{CO}_3)_2$] matrix.²⁷ Semiquantitative values of Ca ranged from below detection limits up to 9%. Previous archaeometric studies had identified Ca as a discriminatory element for this site.

From previous analyses, Bookartoo is known for its relatively high Fe, Ca and V concentrations.²⁷ The microelemental analysis supports these conclusions from the bulk chemical analyses, however the concentration and distribution across the samples is not consistent. Karrku, Moana and Pine Point have very little Ca, however Wilgie Mia has Ca associated with both small rounded and large angular particles. There is a direct correlation between the Fe and Ca in both Bookartoo and Wilgie Mia samples suggesting that during deep weathering of the sites the Fe oxides may have reacted with the dolomite or

1 calcite to form ankerite ($\text{CaFe}(\text{CO}_3)_2$, the Fe analogue of
2 dolomite.^{16, 31, 32}

3
4 While not exhaustive of every site in Australia these results
5 suggest that Ca is indicative with banded iron formations within
6 covered deposits or related formations, and not as associated
7 with weathered, exposed sites. For this sample set, Ca is one of
8 a few clear discriminatory elements for Bookartoo and Wilgie
9 Mia and is characteristic of these sites in higher concentrations.
10

11 *Figure 5: Microelemental map of Rb for samples from the sites*
12 *analysed in this study. Images are false coloured to*
13 *demonstrate relative concentration intensities, with black the*
14 *lowest and white/yellow the highest. Sites are highlighted in*
15 *each image. (a)Bookartoo (b) Karrku (c) Moana (d)Pine Point*
16 *(e)Wilgie Mia*
17

18 Rb

19 Rb was an element that ranged from below detection limits to
20 212 ppm in the sites examined, and was detected in most of the
21 samples analysed. (Table 1)
22

23 However, essentially very little Rb was identified in the
24 Bookartoo or Wilgie Mia ochre samples, and therefore it is not
25 associated with Fe or other Fe-bearing minerals from the site.
26

27 Moana has variability with the samples in the concentration of
28 Rb. The higher concentrations of Rb appear to be associated
29 with larger, angular particles rather than smaller rounded
30 particles. Similarly to Moana, Karrku also has Rb associated
31 with the larger angular particles, but this is not universally
32 found across all samples from the site.
33

34 Pine Point ochre samples have some distribution of Rb,
35 particularly in the larger particles in samples OCH302, 303
36 and 304, which represent a particular sampling location within the
37 site. OCH 309 and 310, 299 and 048 do not have the same
38 distribution of Rb, reflecting the diversity of the ochre material
39 within the site.
40

41 Other elements

42 Images of elemental maps of the slides with elements that were
43 less consistently observed will not be discussed as extensively
44 as the above elements. These include As, Ti and Mn.
45

46 For As, most samples are devoid of even low concentrations of
47 As, with the exception of OCH254-A, OCH101-C and
48 OCH275-C from Moana. As discussed earlier, these samples
49 may be related to the archaeology of the site rather than being
50 examples of source samples.
51

52 Ti is not in high concentration or distribution for the sites with
53 the exception of Wilgie Mia. The amount of Ti in the sample is
54 not necessarily related to the sampling campaign for these. Of
55

56 these samples, OCH062, 062-A and 063, 067, 065 (Western
57 Australia Museum) and 119, 117-Y, 117-A and 119 (Mike
58 Smith) have relatively high concentrations of Ti. However,
59 OCH 260 (Mike Smith) and 065-A (WA Museum) do not. As
60 discussed earlier, this reflects the large scale of the site and the
possibilities of the sampling locations. Titanium can occur at
low levels in hematite, but can also be present as one of the
 TiO_2 polymorphs of are ilmenite (FeTiO_3), which are
widespread detrital minerals in sediments.

Both Cr and Mn have similar distributions patterns to Fe in the
ochre samples, with similar trends in concentration and
distribution. This indicates they are present substituting into
hematite and magnetite. The distributions of these elements will
not be discussed in depth.,

61 Tri-elemental images

62 One of the strengths of the XFM technique combined with
63 GeoPIXE is the ability to generate elemental maps of three
64 elements simultaneously. This “overlying” of elemental maps
65 allows clear differentiation of correlation and anti-correlation of
66 elements as well as the relationship of elemental concentration
67 to a particle or particles or features in the sample. As with the
68 single element plots, the individual elements are falsely
69 coloured to indicate concentration intensity. Using the three
70 colours of red, green and blue, the elements can be easily
71 identified as well as mixtures (e.g. equal amounts of red and
72 blue generate purple regions). As there were many
73 combinations of elements, the combination of Ca (red), Fe,
74 (green) and V (blue) was a representative example.
75

76 *Figure 6: Microelemental map of Ca, Fe and V for samples*
77 *from the sites analysed in this study. Red indicates Ca, green*
78 *indicates Fe and blue indicates V. Images are false coloured to*
79 *demonstrate relative concentration intensities, with black the*
80 *lowest and the indicated colour the highest. Sites are*
81 *highlighted in each image.*
82

83 *(a)Bookartoo (b) Karrku (c) Moana (d)Pine Point (e)Wilgie*
84 *Mia*

85 Visualising the samples in this context allows more
86 interpretation of the elemental distribution for each sample
87 type. In this combination, Karrku, Moana, Pine Point and
88 Wilgie Mia generally are composed of varying concentrations
89 of Fe. However, Bookartoo is revealed to be a complex
90 mixture of Ca, Fe and V, especially in cases such as OCH 255-
91 2 and 255-4 where elemental concentrations can be attributed to
92 individual particles. Moana samples OCH 254, 281 and 275 as
93 attribution case study examples provide a revealing story. The
94 tri-elemental plots allow for characterisation using three
95 discriminatory elements. Moana does not necessarily have a
96 clear elemental profile or definition; rather three to four
97 patterns are seen in the particle size and elemental
98 concentrations. As seen at the site itself, Moana is a large
99 distribution of red and yellow formations with differing
100

1 characteristics. Unlike Bookartoo, the diversity of the Moana
2 site makes it more difficult to attribute an archaeological
3 “unknown” to the site, whereas this attribution would be easier
4 with a sample from Bookartoo or Wilgie Mia.

5
6 *Figure 7: Microelemental map of Ca, Fe and V for all 165*
7 *samples analysed in this study. Red indicates Ca, green*
8 *indicates Fe and blue indicates V. Images are false coloured to*
9 *demonstrate relative concentration intensities, with black the*
10 *lowest and the indicated colour the highest.*

11
12 Figure 7 displays the tri-elemental plot of Ca, Fe and V for all
13 165 elements analysed. These data represent a large variety of
14 deposits and sites from across Australia. This figure
15 demonstrates the great diversity of deposit chemistry and
16 particle distribution and sizes.

17 Light Microscopy

18
19 *Figure 8: Transmitted light microscopy of the same slides*
20 *analysed by XFM at 100x magnification. The scale bar is 200*
21 *micron for each image. Images are arranged in the same*
22 *order, as on the slide. (a)Slide A1 (b)Slide A2 (c) Slide A3*
23 *(d)Slide B1*

24
25 With visual inspection of the slides it can be observed that for
26 several samples there is a very low amount of ochre sample
27 within the epoxy resin. Therefore the elemental maps with low
28 concentrations of Fe are more representative of the relatively
29 few particles of ochre rather than a low concentration of a
30 particular element in the particles. This relatively low
31 concentration may be a reflection of the properties of mixing of
32 the material with the resin; therefore mixing of the same
33 material with another traditional paint binder such as water,
34 natural resin, or proteinaceous binder may have a different
35 effect on the number of particles in suspension.⁴ In addition, as
36 all samples were pre-sieved to less than 250 micron, it may be
37 the case that the ochre samples from these sites have more
38 particles larger than 250 micron.

39
40 The colour of the individual ochre sample can also be observed
41 for each sample. Most examples are in the traditional palette of
42 reds, oranges, yellows and browns and even some purple
43 samples. The colour and particle shape variability can also be
44 observed within the individual samples and between samples
45 from the same site. For instance, OCH024 and 255-A (B1)
46 demonstrate the deep red colour and mixture of intense fine
47 particles (5-10 micron) along with the larger “platy” dark
48 particles (200 micron) characteristic of the site. However,
49 OCH 101-C (A2, Moana) contains a collection of yellow
50 spherical particles on the order of 50-100 micron. The particle
51 colour as well as the shape influence the overall colour when
52 viewed by eye, and the elemental composition (in combination
53 with lighter elements such as Ca, O, Si, K and others form the
54 original mineralogy of the material. Viewing this microscopic
55 palette of the 165 samples analysed in this study gives a

comprehensive view into the diversity of minerals and mineral
mixtures that compose Australian ochre.

Conclusions

This study demonstrates the first successful use of X-ray
fluorescence microanalysis towards the characterisation of
multiple Australian Aboriginal ochre samples from across
Australia. Samples from cultural areas including both sources
and archaeological contexts provide a wide-ranging data set to
examine the variability within and between site locations. The
micron-scale elemental maps produced in this work provide
compositional and spatial information on the distribution of
minerals in complex pigment materials that are not available in
bulk techniques. The results from this study support earlier
bulk technique data on the elemental characterisation of ochre
samples, and supports the need for sensitive multielemental
techniques to fully understand this complex and variable
material. Semiquantitative data from GeoPIXE also aids in
understanding elemental trends in the samples for a
standardised area on a sample slide.

As each sample is representative of a small area of an ochre
source with inherent variability due to genesis and site history,
one sample from each site cannot be considered representative
of a large site location. As demonstrated in this study, some
sites such as Bookartoo the deposits are relatively consistent,
whereas for a site such as Moana where digenic processes
have altered the site has a more diverse elemental and mineral
profile. Rather, the combination of source samples using
multiple elements allows characterisation down to the
association of elemental profile with single particles. In
addition, the presence or absence of a single element is not
indicative of a particular source location; rather a combination
of elements and concentrations as well as elements relative to a
particular particle pattern aid in the characterisation of the
material from a particular site. The addition of light
microscopy of the same areas elementally analysed provides a
fuller picture of the particle colours and distribution. This
study assists in the attribution of ochre to original sites, aiding
in the understanding of the cultural uses and potential exchange
of ochre, however assignments of samples to particular cultural
locations must be made with care and with an understanding of
both the chemistry and cultural context. Future studies include
expansion of the database of deposits and archaeological sites
and application to artefacts.

Acknowledgements

We gratefully acknowledge the South Australian Museum
Board and South Australian Museum Aboriginal Advisory
Group for support and permission to access and analyse the
collections. We also thank the staff at the South Australian
Museum Aboriginal Australian Collections for access to the
collections. We are also grateful to Mike Smith and other
collaborators for access to their collections for analysis. We
acknowledge the preparation of the epoxy cast samples by Ms.

Caroline Watson and Mr. Owen Osborne. The staff at Pontifex, Kensington, South Australia are gratefully acknowledged for their careful final preparation of the slides. We acknowledge Professor Paul Kirkbride, Flinders University for the use of the microscope. The project has approval number 4670 from the Social and Behavioural Research Ethics Committee of Flinders University. Funding is gratefully acknowledged from Australian Institute of Nuclear Science and Engineering (AINSE) Research Fellowship (Popelka-Filcoff), and Australian Research Council Grant #LP0882597 (Lenehan, Pring and Popelka-Filcoff). Part of this research was undertaken on the XFM beam line at the Australian Synchrotron, Victoria, Australia.

Notes and references

^a School of Chemical and Physical Sciences, Flinders University, Adelaide, SA Australia

^b Centre for Environmental Risk Assessment and Remediation, University of South Australia, Adelaide, SA Australia

^c Australian Synchrotron, Clayton, VIC Australia.

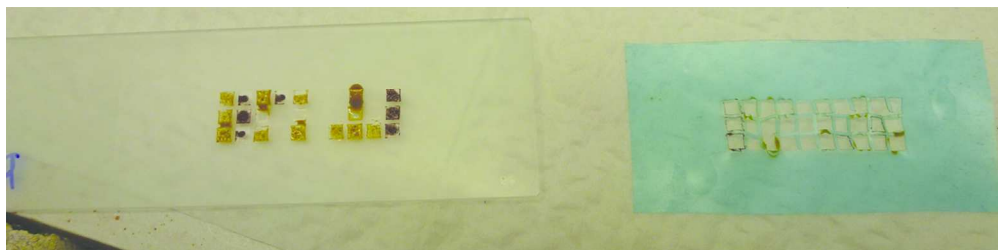
^d South Australian Museum, Adelaide, SA Australia

1. P. Nel, P. A. Lynch, J. S. Laird, H. M. Casey, L. J. Goodall, C. G. Ryan and R. J. Sloggett, *Nuclear Instruments and Methods in Physics Research Section A: Accelerators, Spectrometers, Detectors and Associated Equipment*, 2010, **619**, 306-310.
2. P. S. C. Tacon, in *Soils, Stones and Symbols: Cultural Perceptions of the Mineral World*, ed. N. O. M. A. Boivin, UCL Press, London, Editon edn., 2004, pp. 31-42.
3. A. J. Blee, K. Walshe, A. Pring, J. S. Quinton and C. E. Lenehan, *Talanta*, 2010, **82**, 745-750.
4. T. Reeves, R. S. Popelka-Filcoff and C. E. Lenehan, *Analytica Chimica Acta*, 2013, **803**, 194-203.
5. R. M. Cornell and U. Schewertmann, *The Iron Oxides*, Wiley-VCH Verlag GmbH & Co. , Weinheim, 2003.
6. R. S. Popelka-Filcoff, C. Lenehan, K. Walshe, J. W. Bennett, A. Stopic, P. Jones, A. Pring, J. S. Quinton and A. Durham, *Journal of the Anthropological Society of South Australia*, 2012, **35**.
7. R. S. Popelka-Filcoff, C. E. Lenehan, M. D. Glascock, J. W. Bennett, A. Stopic, J. S. Quinton, A. Pring and K. Walshe, *Journal of Radioanalytical and Nuclear Chemistry*, 2012, **291**, 19-24.
8. R. S. Popelka-Filcoff, A. Mauger, C. E. Lenehan, K. Walshe and A. Pring, *Analytical Methods*, 2014, **6**, 1309-1316.
9. U. Bergmann, P. L. Manning and R. A. Wogelius, in *Annual Review of Analytical Chemistry*, Vol 5, eds. R. G. Cooks and E. S. Yeung, Annual Reviews, Palo Alto, Editon edn., 2012, vol. 5, pp. 361-389.
10. L. Bertrand, L. Robinet, M. Thoury, K. Janssens, S. Cohen and S. Schöder, *Appl. Phys. A*, 2012, **106**, 377-396.
11. D. L. Howard, M. D. de Jonge, D. Lau, D. Hay, M. Varcoe-Cocks, C. G. Ryan, R. Kirkham, G. Moorhead, D. Paterson and D. Thurrowgood, *Analytical Chemistry*, 2012, **84**, 3278-3286.
12. K. Janssens, J. Dik, M. Cotte and J. Susini, *Accounts of Chemical Research*, 2010, **43**, 814-825.
13. L. Monico, G. Van der Snickt, K. Janssens, W. De Nolf, C. Miliani, J. Dik, M. Radepon, E. Hendriks, M. Geldof and M. Cotte, *Analytical Chemistry*, 2011, **83**, 1224-1231.
14. R. L. Green and R. J. Watling, *Journal of Forensic Sciences*, 2007, **52**, 851-859.
15. M. Jercher, A. Pring, P. G. Jones and M. D. Raven, *Archaeometry*, 1998, **40**, 383-401.
16. M. Smith and B. Fankhauser, *Geochemistry and identification of Australian red ochre deposits* National Museum of Australia and Centre for Archaeological Research, Canberra, 2009.
17. R. Scadding, V. Winton and V. Brown, *Journal of Archaeological Science*, 2015, **54**, 300-312.
18. D. C. Creagh, M. E. Kubik and M. Sterns, *Nuclear Instruments and Methods in Physics Research Section A: Accelerators, Spectrometers, Detectors and Associated Equipment*, 2007, **580**, 721-724.
19. P. Jones, *Journal of the Anthropological Society of South Australia* 1984, **22**, 3-10.
20. P. Jones, *Journal of the Anthropological Society of South Australia* 1984, **22**, 10-19.
21. P. Jones, *Ochre and Rust: Artefacts and Encounters on Australian Frontiers*, Wakefield Press Adelaide, 2007.
22. P. Jones and P. Sutton, *Art and Land: Aboriginal Sculptures of The Lake Eyre Region*, South Australian Museum and Wakefield Press, Adelaide, Australia, 1986.
23. M. F. Nobbs, *Aboriginal painters of the Olary District of South Australia an ethnoecological study of the Lake Frome Plains and the adjoining uplands, with particular reference to the granite area of the Olary Uplands / By Margaret Nobbs. --History*, 1995., 1996.
24. R. Popelka-Filcoff, C. Lenehan, M. Glascock, J. Bennett, A. Stopic, J. Quinton, A. Pring and K. Walshe, *Journal of Radioanalytical and Nuclear Chemistry*, 2012, **291**, 19-24.
25. M. A. Smith and B. Fankhauser, *An archaeological perspective on the geochemistry of Australian red ochre deposits: Prospects for fingerprinting major sources*, Australian Institute of Aboriginal and Torres Strait Islander Studies, Canberra, 1996.
26. M. A. Smith and S. Pell, *Journal of Archaeological Science*, 1997, **24**, 773-778.
27. J. L. Keeling, *Geological Survey: Bookartoo Ochre Deposit Sec. 85 HD. Parachilna 831*, Department of Mines and Energy, South Australia, 1984.
28. N. Paterson and R. Lampert, *Records of the Australian Museum*, 1985, **37**, 1-9.
29. J. Clarke, *Studies in Conservation*, 1976, **21**, 134-142.
30. C. G. Ryan, R. Kirkham, R. M. Hough, G. Moorhead, D. P. Siddons, M. D. de Jonge, D. J. Paterson, G. De Geronimo, D. L. Howard and J. S. Cleverley, *Nuclear Instruments and Methods in Physics Research Section A: Accelerators, Spectrometers, Detectors and Associated Equipment*, 2009, **619**, 37-43.
31. J. Clarke and N. North, in *Rock Art and Posterity: Conserving, Managing and Recording Rock Art*, eds. C. Pearson and B. K. Swartz Jr., Australian Rock Art Research Association, Melbourne, Editon edn., 1991, pp. 80-87.
32. J. Clarke and N. North, in *Rock Art and Posterity: Conserving, Managing and Recording Rock Art*, eds. C. Pearson and B. K. Swartz Jr., Australian Rock Art Research Association, Melbourne, Editon edn., 1991, pp. 88-92.

1
2
3
4
5
6
7
8
9
10
11
12
13
14
15
16
17
18
19
20
21
22
23
24
25
26
27
28
29
30
31
32
33
34
35
36
37
38
39
40
41
42
43
44
45
46
47
48
49
50
51
52
53
54
55
56
57
58
59
60

Analytical Methods Accepted Manuscript

1
2
3
4
5
6
7
8
9
10
11
12
13
14
15
16
17
18
19
20
21
22
23
24
25
26
27
28
29
30
31
32
33
34
35
36
37
38
39
40
41
42
43
44
45
46
47
48
49
50
51
52
53
54
55
56
57
58
59
60



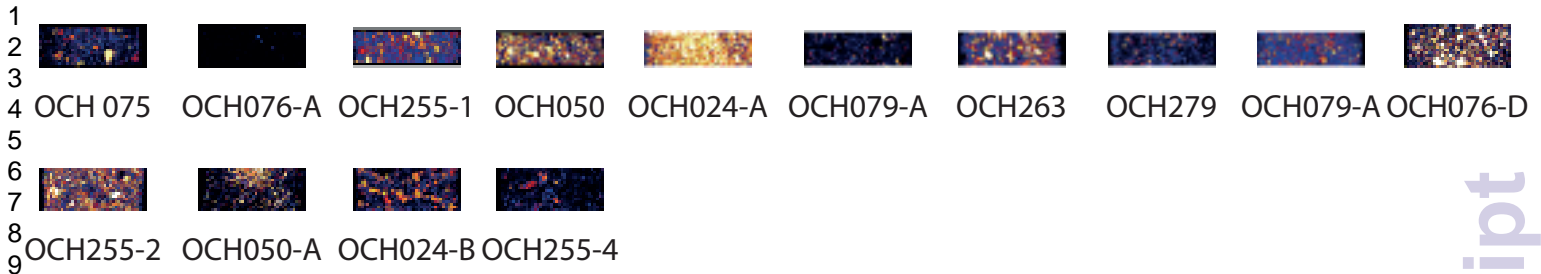
289x71mm (120 x 120 DPI)

1
2
3
4
5
6
7
8
9
10
11
12
13
14
15
16
17
18
19
20
21
22
23
24
25
26
27
28
29
30
31
32
33
34
35
36
37
38
39
40
41
42
43
44
45
46
47
48
49
50
51
52
53
54
55
56
57
58
59
60

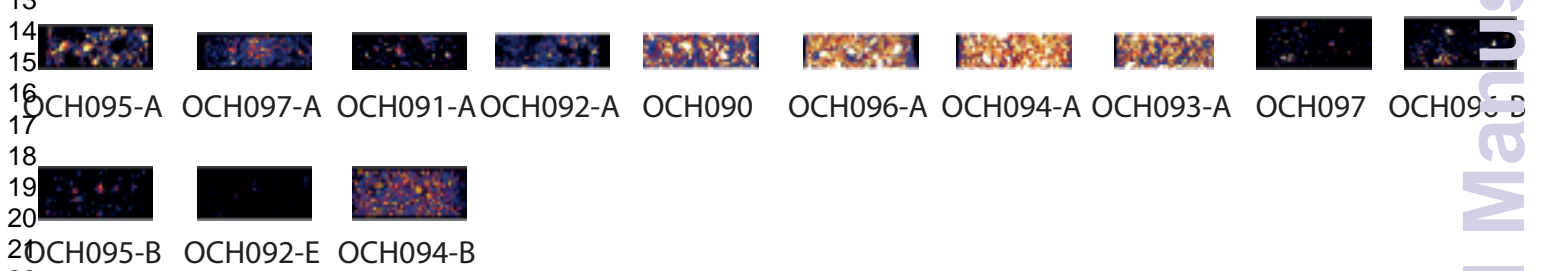


290x217mm (120 x 120 DPI)

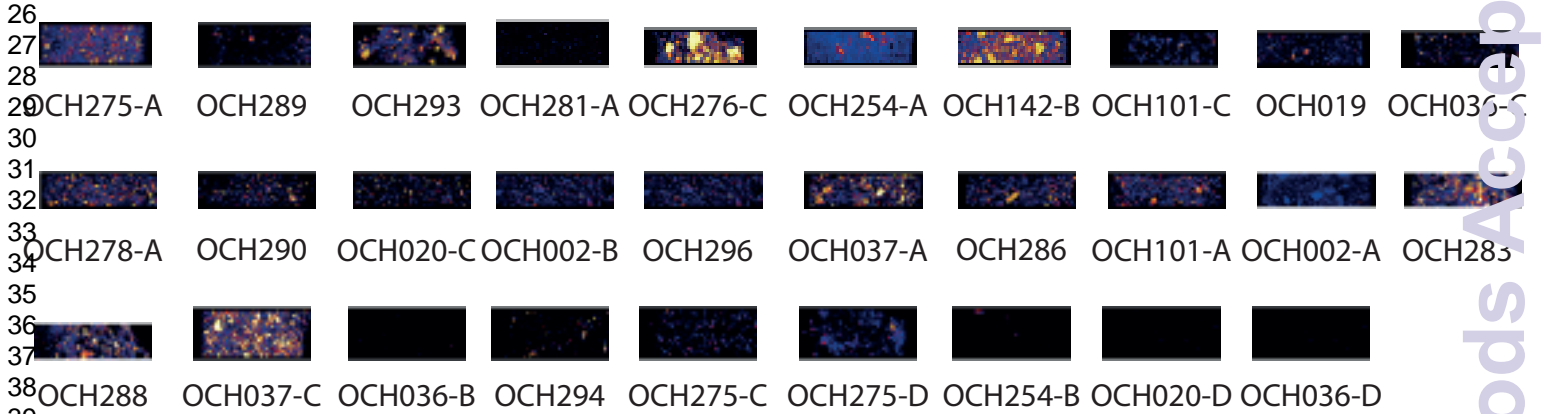
Bookartoo



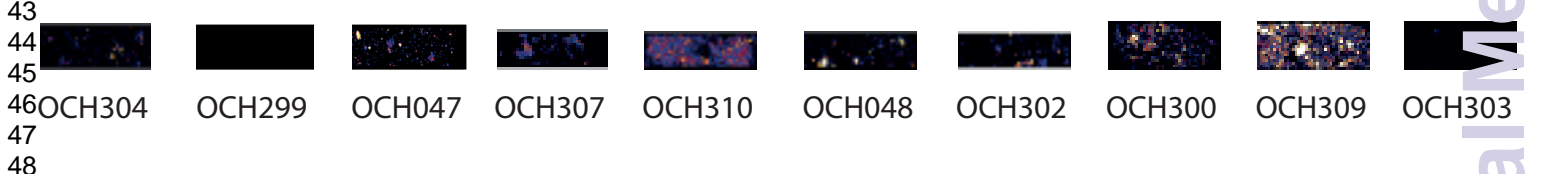
Karrku



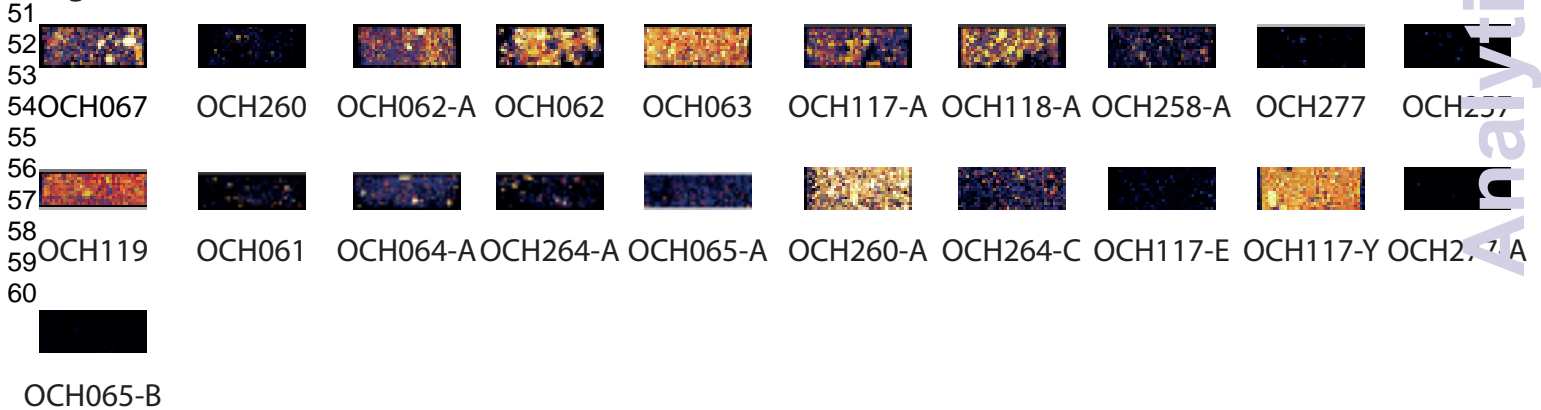
Moana



Pine Point

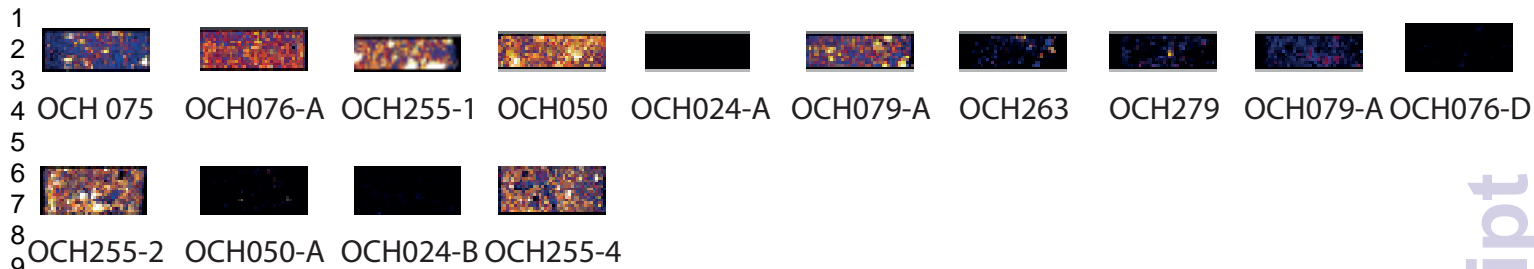


Wilgie Mia

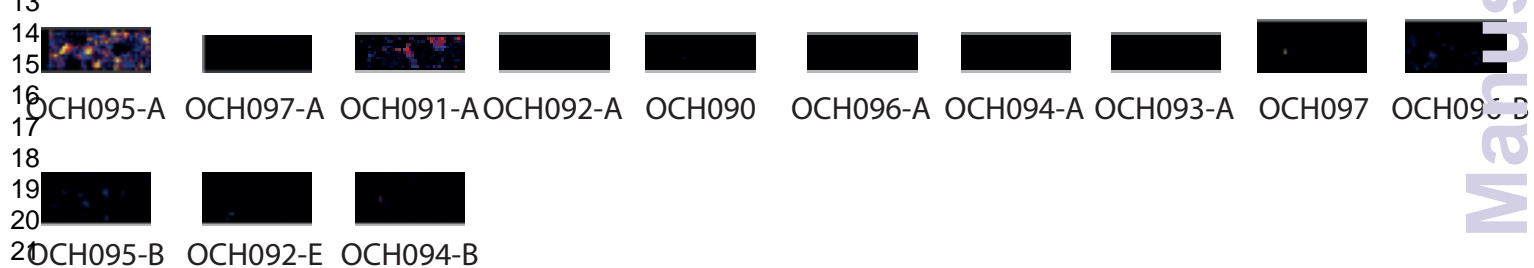


Analytical Methods Accepted Manuscript

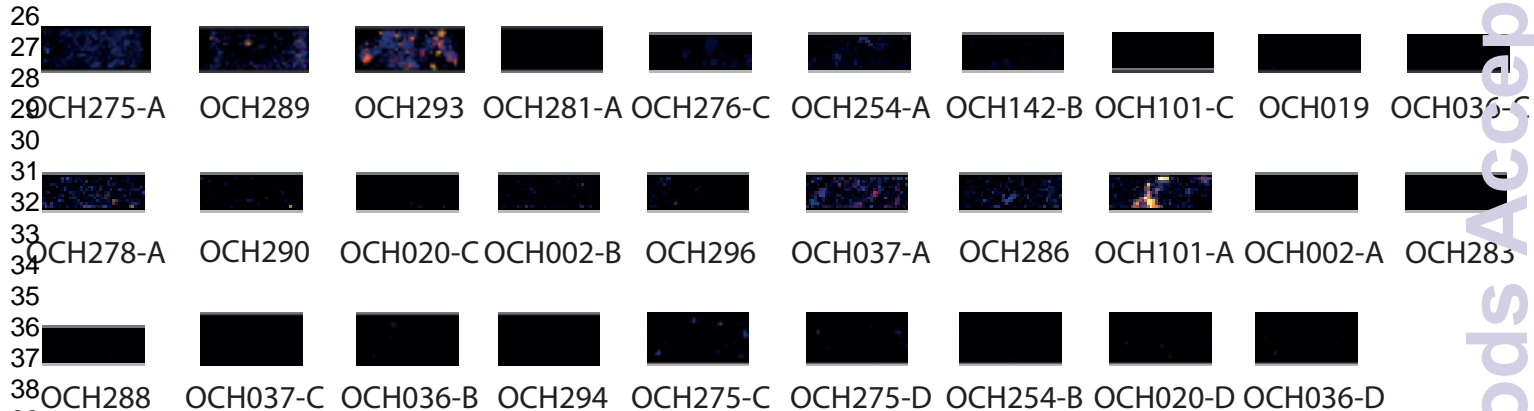
Bookartoo



Karrku



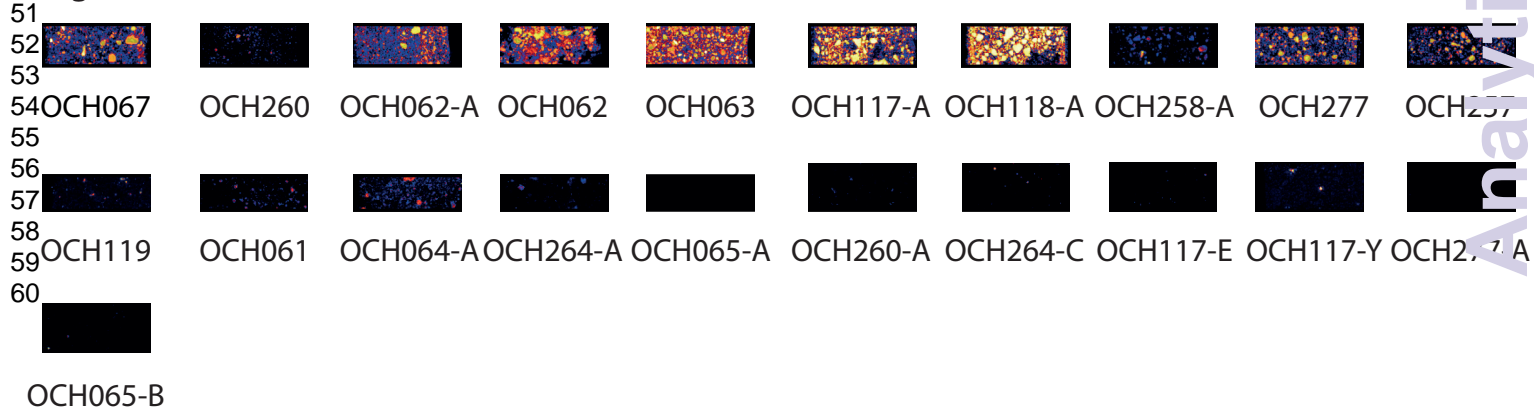
Moana



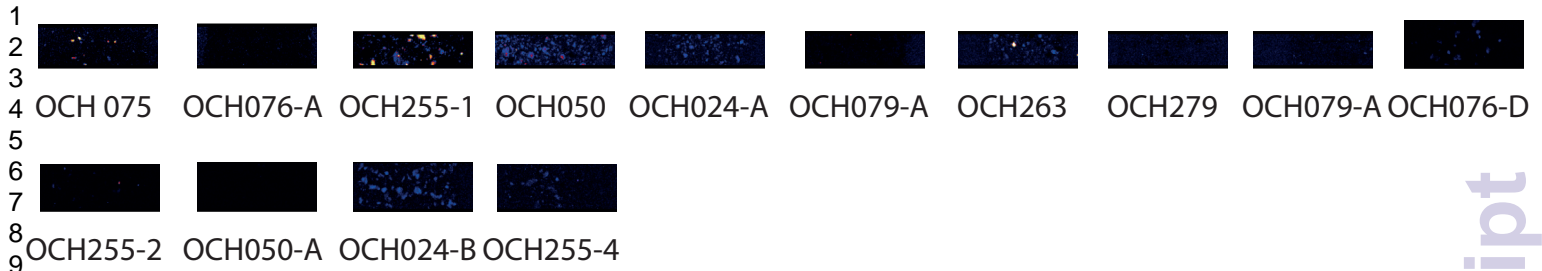
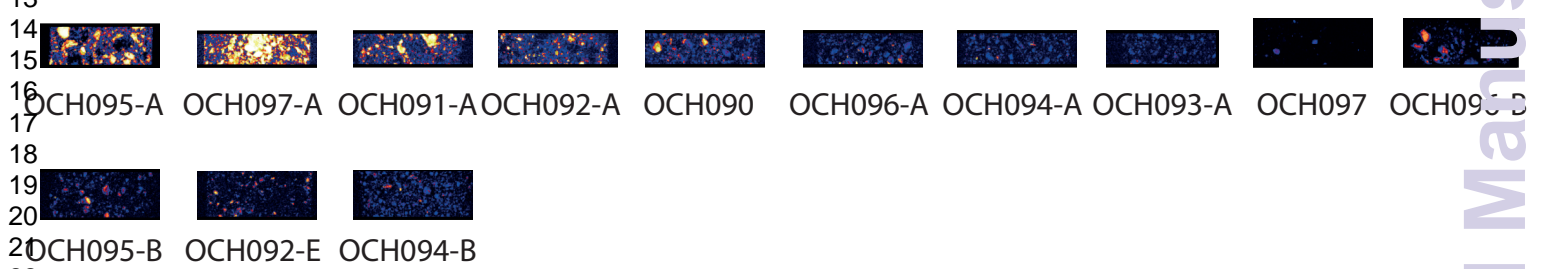
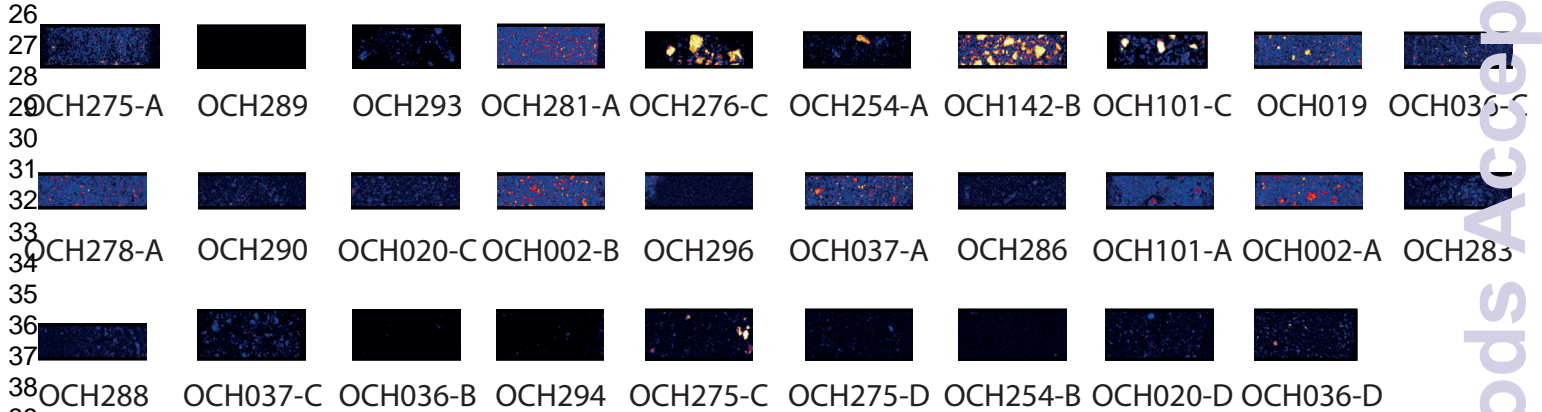
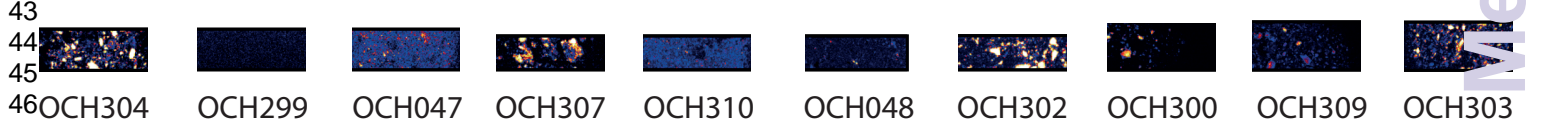
Pine Point



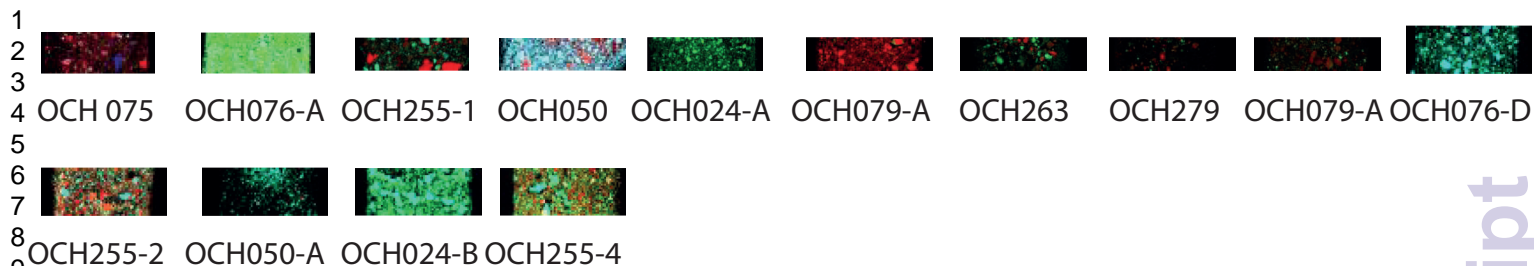
Wilgie Mia



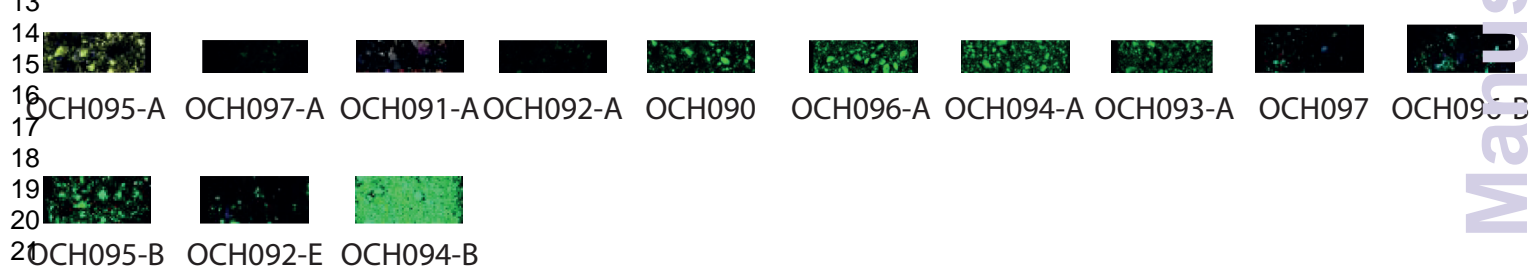
Analytical Methods Accepted Manuscript

Bookartoo**Karrku****Moana****Pine Point****Wilgie Mia**

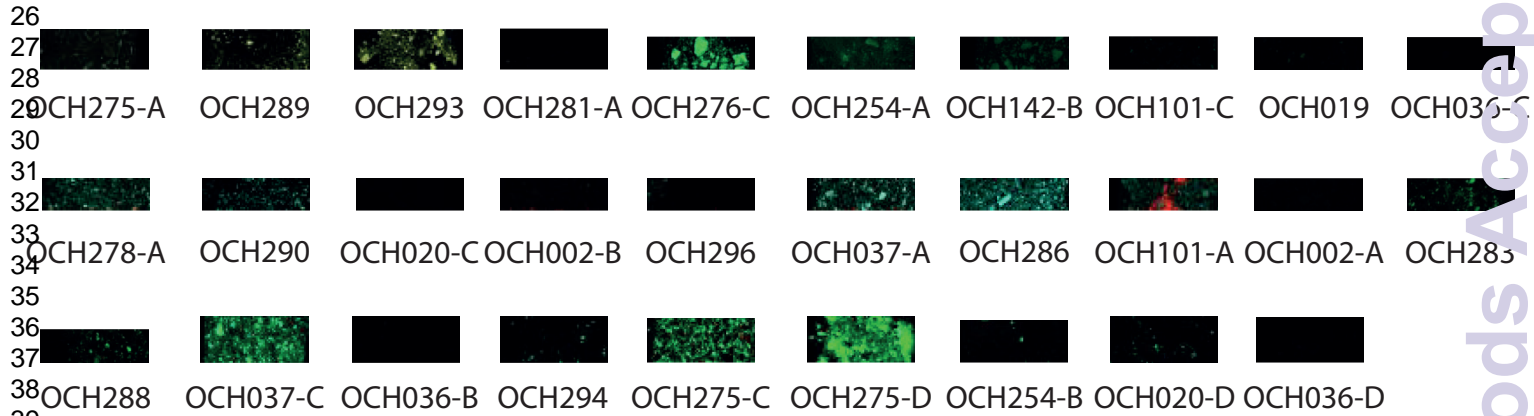
Bookartoo



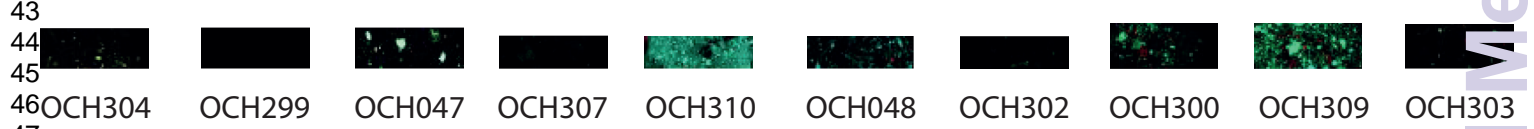
Karrku



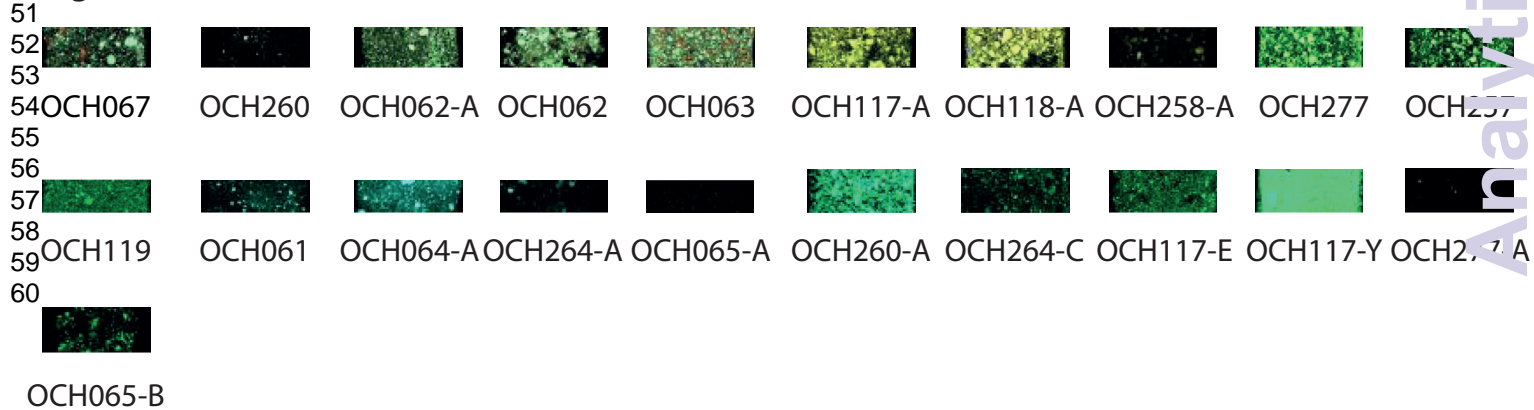
Moana



Pine Point



Wilgie Mia

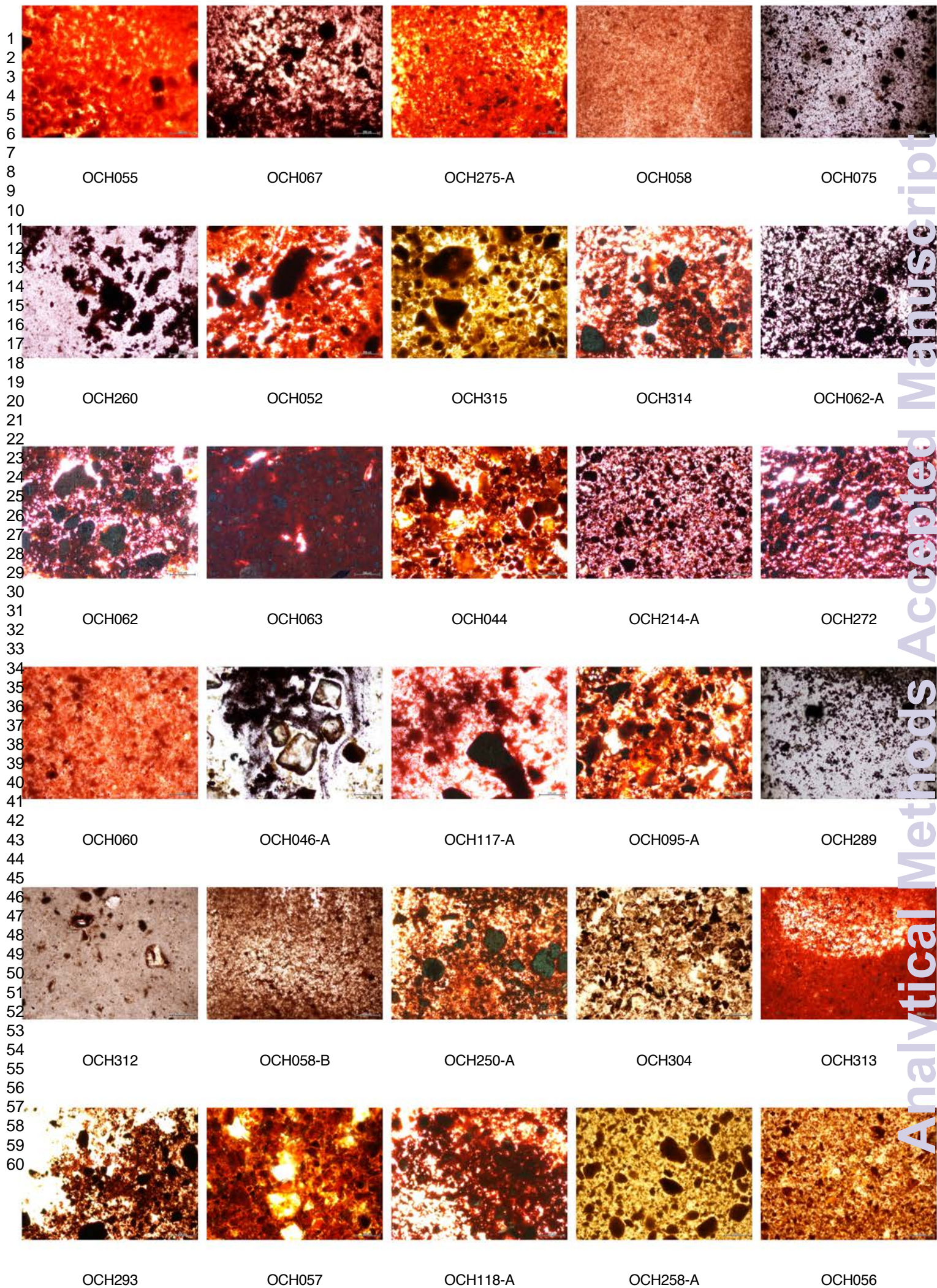


Analytical Methods Accepted Manuscript

1
2
3
4
5
6
7
8
9
10
11
12
13
14
15
16
17
18
19
20
21
22
23
24
25
26
27
28
29
30
31
32
33
34
35
36
37
38
39
40
41
42
43
44
45
46
47

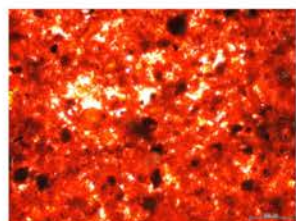
OCH055 Rockleigh	OCH067 Wilgie Mia	OCH275-A Moana	OCH058 Tombstone Dam	OCH075 Bookartoo	OCH260 Wilgie Mia	OCH052 Puttapa Gap	OCH315 Killalpannina	OCH314 Killalpannina	OCH062-A Wilgie Mia	OCH062 Wilgie Mia	OCH063 Wilgie Mia	OCH044 Overland Corner	OCH214-A Mount Hayward	OCH272 Coopers Creek
OCH060 Wangiana	OCH046-A Pernatty Lagoon	OCH117-A Wilgie Mia	OCH095-A Karrku	OCH289 Moana	OCH312 Killalpannina	OCH058-B Tombstone Dam	OCH250-A Mount Hayward	OCH304 Pine Point	OCH313 Killalpannina	OCH293 Moana	OCH057 Bluff Quarry	OCH118-A Wilgie Mia	OCH258-A Wilgie Mia	OCH056 Rockleigh
OCH071 Dongup	OCH249 Mount Hayward	OCH281-A Moana	OCH076-A Bookartoo	OCH051 Puttapa	OCH262 MacDonnell Ranges	OCH250 Mount Hayward	OCH042 Ochre Cliffs	OCH253 Mount Hayward	OCH277 Wilgie Mia	OCH046-B Pernatty Lagoon	OCH248 Mount Hayward	OCH299 Pine Point	OCH257 Wilgie Mia	OCH047 Pine Point
OCH098-B Lawa 98/1	OCH276-C Moana	OCH307 Pine Point	OCH119 Wilgie Mia N-2b	OCH109-A Rockleigh N-8A	OCH254-A Moana	OCH084-B Gara Widgie	OCH255-1 Bukartu	OCH102-B Mount Howden	OCH087 Glen Helen	OCH085 Glen Helen	OCH142-B Moana	OCH098 Lawa 98/1	OCH105 Overland Corner	OCH102-A Mount Howden
OCH115 Ulpanyali	OCH103 Overland Corner	OCH108 Puritjarra	SRM1633b Standard	OCH114 Tulumbunner	OCH100 Lawa 98/3	SRM690 Standard	OCH111 Tirnu	OCH034 Clayton LEBSA	OCH030 Wangiana	OCH025 Puttapa Gap	OCH017 Bulloo Creek	OCH109-B Rockleigh N-8A	OCH021 Ochre Cliffs Lyndhurst	OCH101-C Moana
OCH097-A Karrku	OCH11-B Tirnu	OCH019 Moana	OCH328 Mount Howden	OCH033 Bulloo Creek	OCH028 Tombstone Dam	OCH018 Clayton Leb SA	OCH316 Killalpaninna	OCH317 Killalpaninna	OCH318 Killalpaninna	OCH084-A Gara Widgie	OCH016 Bluff Quarry	OCH036-A Moana	OCH005 Brachina	OCH040 Ochre Cliffs
OCH278-A Moana	OCH290 Moana	OCH050 Pukatoo	OCH061 Wilgie Mia	OCH064-A Wilgie Mia	OCH091-A Karrku 96/1	OCH020-C Moana Sample 2	OCH002-B Moana	OCH296 Moana	OCH264-A Wilgie Mia	OCH037-A Moana	OCH310 Pine Point	OCH286 Moana	OCH101-A Moana	OCH048 Pine Point
OCH024-A Pukatoo	OCH002-A Moana	OCH079-A Bookartoo	OCH283 Moana	OCH263 Bookartoo	OCH302 Pine Point	OCH092-A Karrku 96/2	OCH288 Moana	OCH090 Karrku #6	OCH279 Bookartoo	OCH096-A Karrku 98/5	OCH094-A Karrku 98/3	OCH065-A Wilgie Mia	OCH079-A Bookartoo	OCH093-A Karrku 98/2
OCH498 Unknown	OCH492 Swanport	OCH504 Ooldea	OCH524 Unknown	OCH526 Mt Davenport	OCH495 Unknown	OCH500 Princess Charlotte Bay	OCH519 Cooper Creek	OCH532 Unknown	OCH496 Tiwi Islands	OCH505 Western NSW	OCH514 Cooper Creek	OCH527 MacDonnell Ranges	OCH533 Unknown	OCH529 Cooper Creek
OCH525 Port Darwin	OCH513 Mornington Island	OCH503 Unknown	OCH260-A Wilgie Mia	OCH076-D Bookartoo	OCH097 Karrku	OCH264-C Wilgie Mia	OCH300 Pine Point	OCH255-2 Bukartu	OCH037-C Moana	OCH-036-B Moana	OCH294 Moana	OCH309 Pine Point	OCH050-A Pukatoo	OCH096-B Karrku
OCH275-C Moana	OCH95-B Karrku	OCH303 Pine Point	OCH117-E Wilgie Mia	OCH275-D Moana	OCH092-E Karrku	OCH024-B Pukatoo	OCH254-B Moana	OCH117-Y Wilgie Mia	OCH277-A Wilgie Mia	OCH255-4 Bukartu	OCH065-B Wilgie Mia	OCH094-B Karrku	OCH020-D Moana	OCH036-C Moana

Analytical Methods Accepted Manuscript

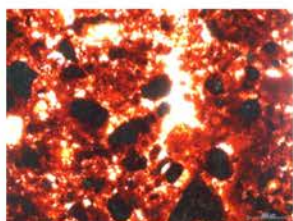


Accepted Manuscript

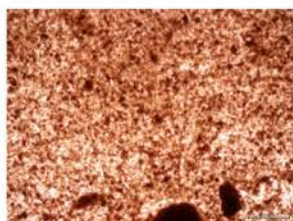
1
2
3
4
5
6
7
8
9
10
11
12
13
14
15
16
17
18
19
20
21
22
23
24
25
26
27
28
29
30
31
32
33
34
35
36
37
38
39
40
41
42
43
44
45
46
47
48
49
50
51
52
53
54
55
56
57
58
59
60



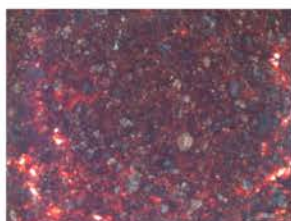
OCH071



OCH249



OCH281-A



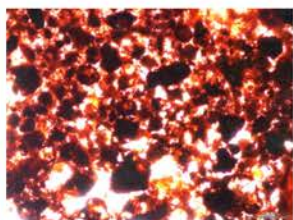
OCH076-A



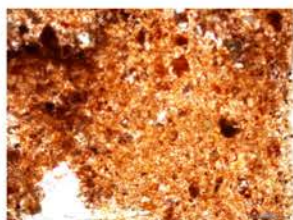
OCH051



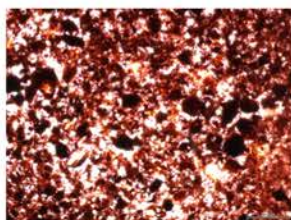
OCH262



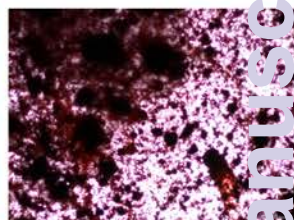
OCH250



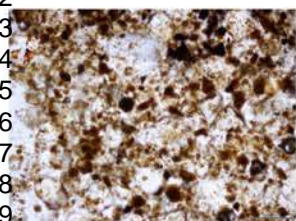
OCH042



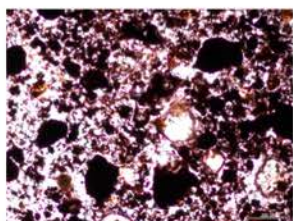
OCH253



OCH277



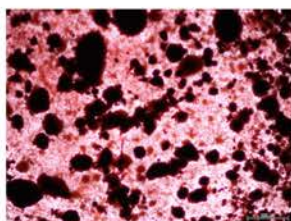
OCH046-B



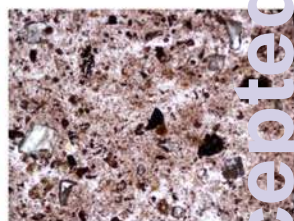
OCH248



OCH299



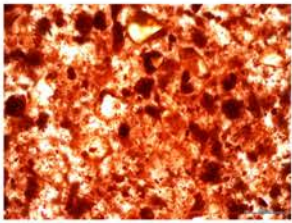
OCH257



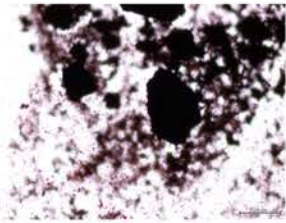
OCH047

Analytical Methods Accepted Manuscript

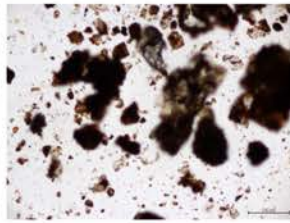
1
2
3
4
5
6
7
8
9
10
11
12
13
14
15
16
17
18
19
20
21
22
23
24
25
26
27
28
29
30
31
32
33
34
35
36
37
38
39
40
41
42
43
44
45
46
47
48
49
50
51
52
53
54
55
56
57
58
59
60



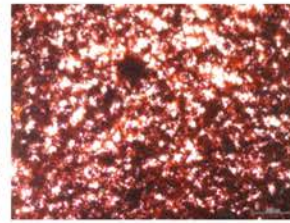
OCH098-B



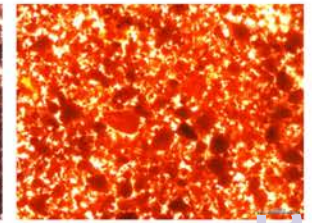
OCH276-C



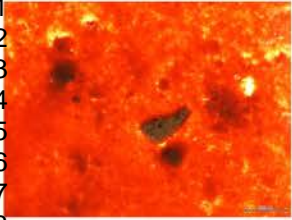
OCH307



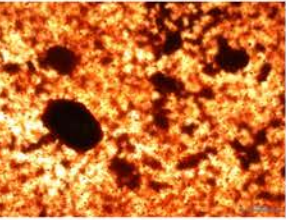
OCH119



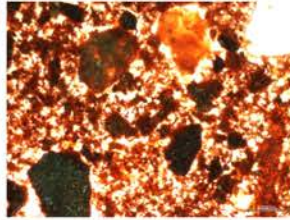
OCH109-A



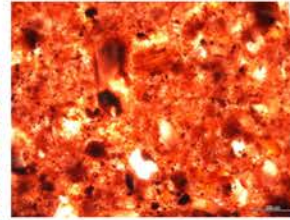
OCH254-A



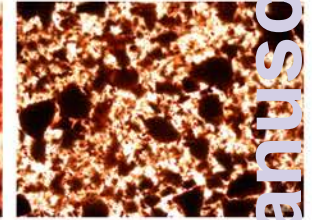
OCH084-B



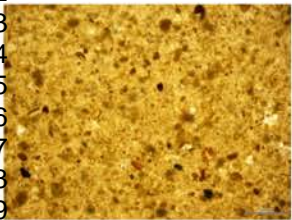
OCH255-1



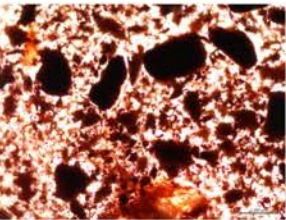
OCH102-B



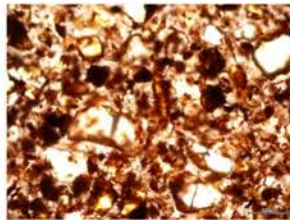
OCH087



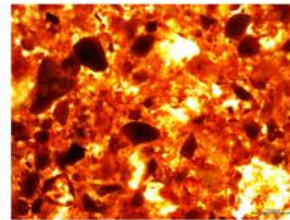
OCH085



OCH142-B



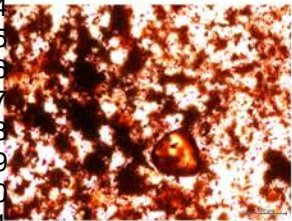
OCH098



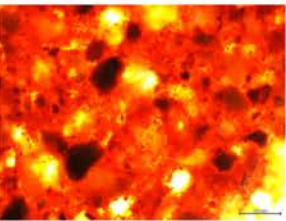
OCH105



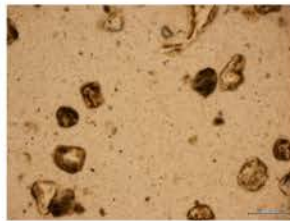
OCH102-A



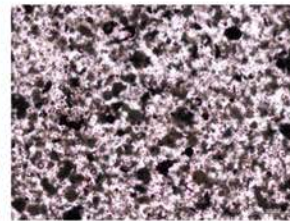
OCH115



OCH103



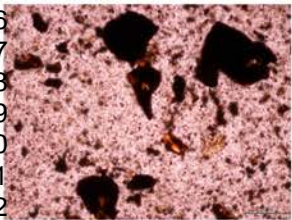
OCH108



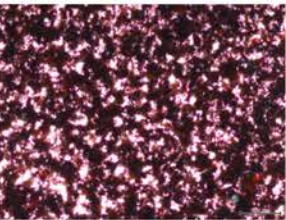
SRM1633B



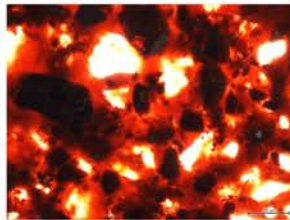
OCH114



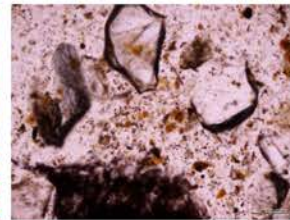
OCH100



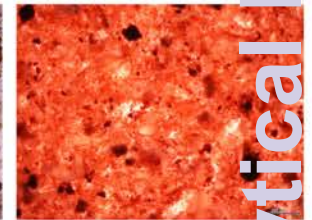
SRM690



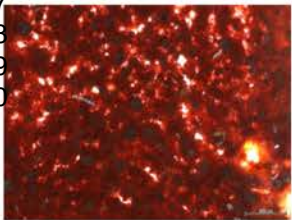
OCH111



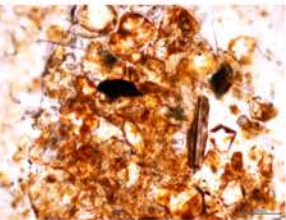
OCH034



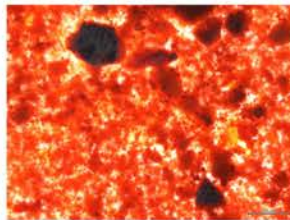
OCH030



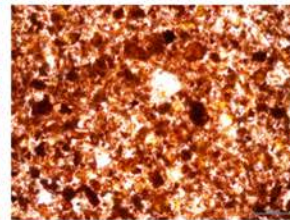
OCH025



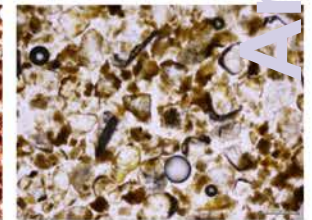
OCH017



OCH109-B



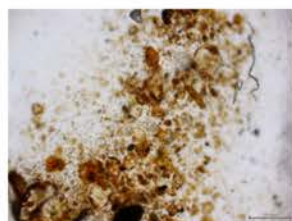
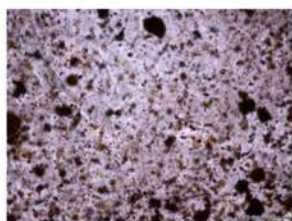
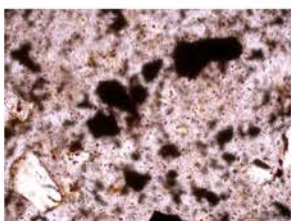
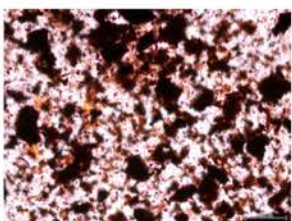
OCH021



OCH101-C

Accepted Manuscript

1
2
3
4
5
6
7
8
9
10
11
12
13
14
15
16
17
18
19
20
21
22
23
24
25
26
27
28
29
30
31
32
33
34
35
36
37
38
39
40
41
42
43
44
45
46
47
48
49
50
51
52
53
54
55
56
57
58
59
60



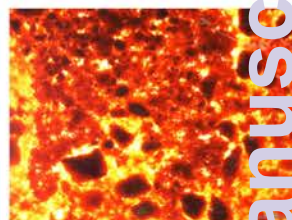
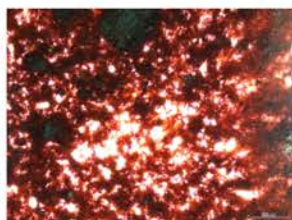
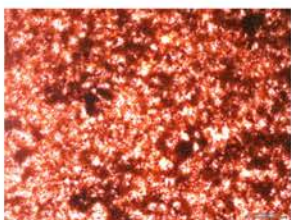
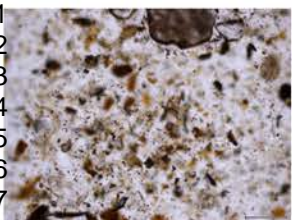
OCH097-A

OCH111-B

OCH019

OCH033

OCH028



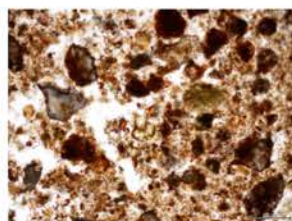
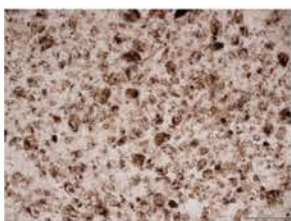
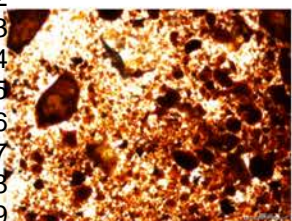
OCH018

OCH316

OCH317

OCH318

OCH084-A



OCH016

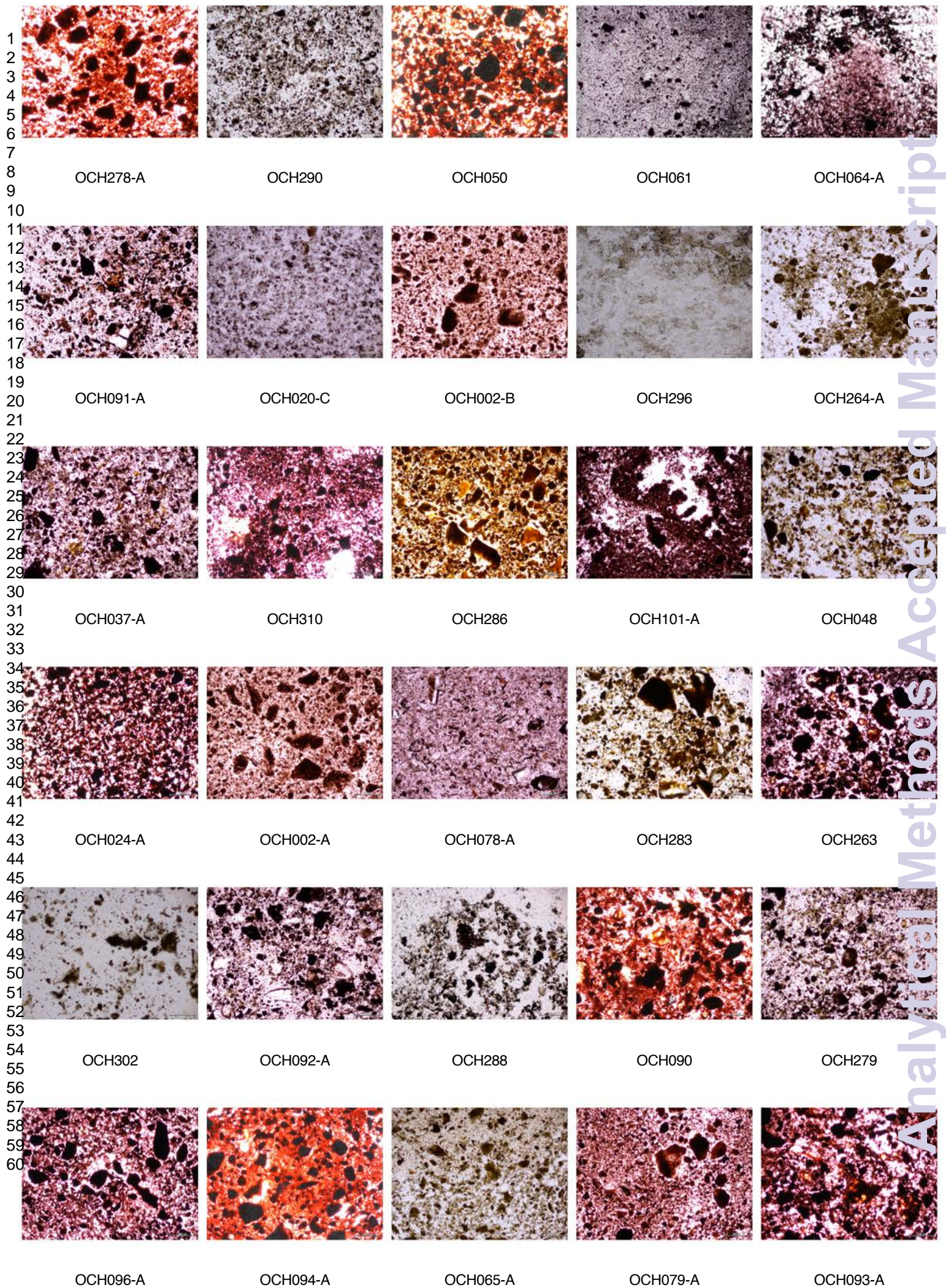
OCH036-A

OCH005

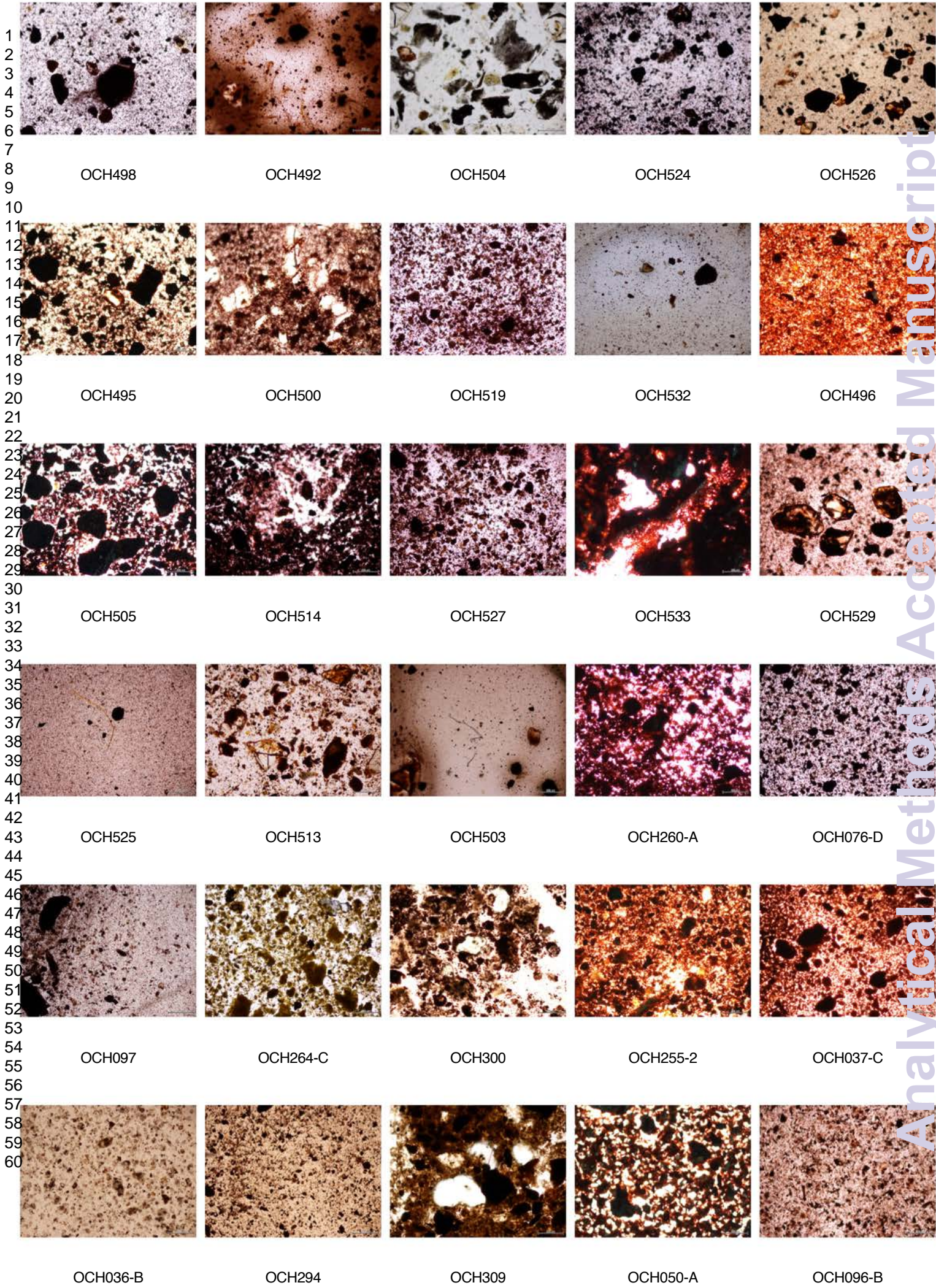
OCH040

OCH328

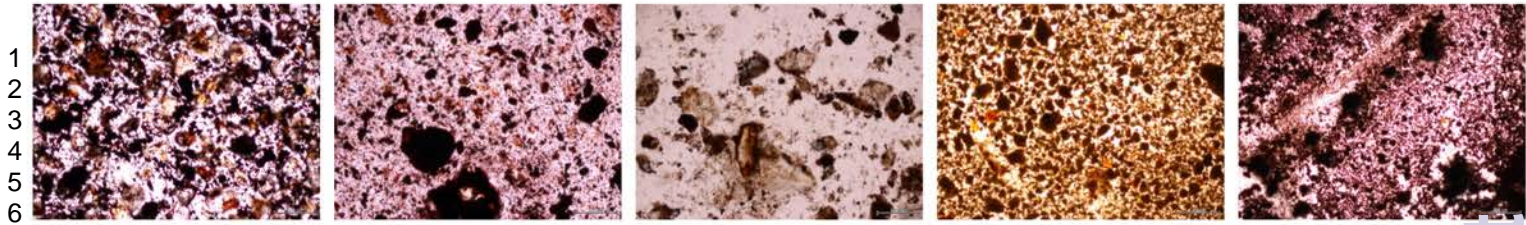
Analytical Methods Accepted Manuscript



Accepted Manuscript



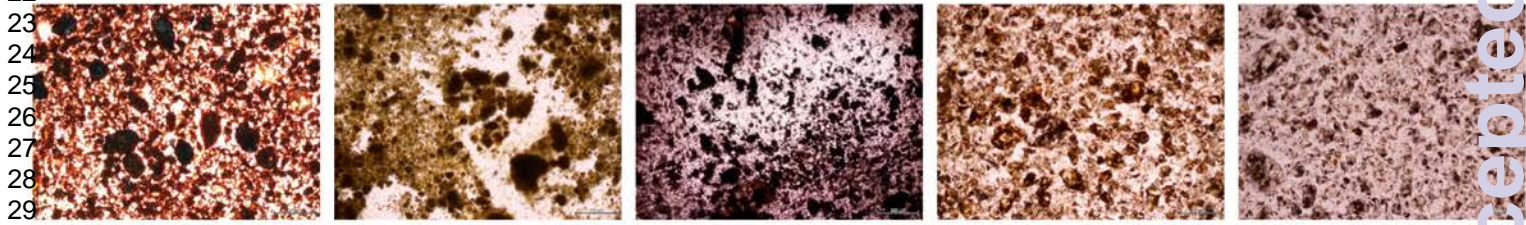
Accepted Manuscript



1
2
3
4
5
6
7
8 OCH275-C OCH095-B OCH303 OCH117-E OCH275-D
9



10
11
12
13
14
15
16
17
18
19 OCH092-E OCH024-B OCH254-B OCH117-Y OCH277-A
20



21
22
23
24
25
26
27
28
29
30
31 OCH255-4 OCH065-B OCH094-B OCH020-D OCH036-C
32

33
34
35
36
37
38
39
40
41
42
43
44
45
46
47
48
49
50
51
52
53
54
55
56
57
58
59
60

ID	Site	Ca	Ca LOD	Sc	Sc LOD	Ti	Ti LOD	V	V LOD	Cr	Cr LOD	Mn	Mn LOD	Fe
OCH075	Bookartoo	33081	35	<LOD	9	232	4	<LOD	2	<LOD	1	1325	3	33350
OCH076-A	Bookartoo	46454	43	<LOD	10	1299	6	551	4	299	2	7989	8	180716
OCH078-A	Bookartoo	9315	86	4	22	1703	5	1373	2	374	1	22758	4	251427
OCH263	Bookartoo	<LOD	39	263	11	810	5	529	3	213	2	17044	7	175920
OCH279	Bookartoo	<LOD	37	<LOD	10	566	4	<LOD	2	<LOD	1	2688	4	25931
OCH079-A	Bookartoo	1800	51	<LOD	14	829	5	<LOD	2	<LOD	2	5040	5	48047
OCH076-D	Bookartoo	<LOD	8	<LOD	4	101	3	209	2	128	1	1745	3	59089
OCH255-1	Bukartu	89638	60	<LOD	17	1625	7	633	4	187	3	17226	10	189012
OCH255-4	Bukartu	18719	23	<LOD	7	222	3	267	2	142	1	2076	4	62840
OCH255-2	Bukartu	23185	26	<LOD	7	130	3	146	2	95	1	1515	3	49260
OCH095-A	Karrku	13693	24	<LOD	7	701	4	<LOD	2	<LOD	1	4937	5	68427
OCH095-B	Karrku	<LOD	8	<LOD	3	84.4	2	<LOD	1	51.4	0.9	937	3	33647
OCH092-E	Karrku	<LOD	6	<LOD	3	<LOD	2	<LOD	1	<LOD	0.7	112	1	7100
OCH094-B	Karrku	789	11	99	6	695	4	533	3	433	2	4730	5	161845
OCH097	Karrku	<LOD	6	<LOD	3	<LOD	2	<LOD	0.9	<LOD	0.6	99.3	1	6676
OCH096-B	Karrku	355	8	<LOD	3	121	2	<LOD	1	<LOD	0.8	312	2	13431
OCH090	Karrku #6	<LOD	16	<LOD	8	<LOD	6	<LOD	3	<LOD	2	374	8	4847
OCH091-A	Karrku 96/1	<LOD	16	<LOD	5	295	3	<LOD	2	<LOD	1	2948	3	28343
OCH092-A	Karrku 96/2	<LOD	13	<LOD	5	841	4	<LOD	2	<LOD	1	418	4	5849
OCH093-A	Karrku 98/2	<LOD	15	398	8	1336	6	<LOD	3	<LOD	2	3671	8	35411
OCH094-A	Karrku 98/3	159	16	49	8	904	6	363	4	253	3	15463	9	146188
OCH096-A	Karrku 98/5	<LOD	16	189	8	1252	6	45	4	28.9	3	7168	9	70166
OCH097-A	Karrku JW	<LOD	14	<LOD	8	1098	5	<LOD	3	<LOD	2	4603	5	41880
OCH062-A	Little Wilgie Mia	32545	35	<LOD	8	820	5	80	3	247	2	6945	7	157272
OCH062	Little Wilgie Mia	41302	39	<LOD	9	1125	6	157	3	337	2	8134	7	191268
OCH275-A	Moana	8852	21	<LOD	6	664	4	<LOD	2	<LOD	1	1298	3	33322
OCH289	Moana	3324	15	<LOD	5	<LOD	3	<LOD	1	<LOD	1	1839	3	25285
OCH293	Moana	10554	22	<LOD	6	575	4	<LOD	2	<LOD	1	4071	5	55829
OCH281-A	Moana	2134	14	<LOD	5	379	3	<LOD	1	<LOD	0.9	220	2	8618

1																
2																
3																
4	OCH278-A	Moana	<LOD	20	<LOD	6	910	4	<LOD	2	9.8	1	6152	4	60005	
5	OCH290	Moana	<LOD	15	<LOD	5	632	3	<LOD	1	<LOD	1	3701	3	36440	
6	OCH002-B	Moana	<LOD	13	<LOD	5	554	3	<LOD	1	<LOD	0.9	1444	2	14622	
7	OCH296	Moana	<LOD	9	<LOD	3	<LOD	2	<LOD	1	<LOD	0.7	374	1	4847	
8	OCH037-A	Moana	<LOD	20	189	6	1252	4	45	2	28.9	1	7168	4	70166	
9	OCH286	Moana	<LOD	23	<LOD	6	453	4	214	2	88	1	9979	5	99019	
10	OCH101-A	Moana	1800	17	<LOD	5	829	3	<LOD	2	<LOD	1	5040	3	48047	
11	OCH002-A	Moana	<LOD	14	<LOD	6	632	5	<LOD	2	<LOD	1	3701	3	36440	
12	OCH283	Moana	<LOD	13	<LOD	7	50	5	72.3	2	19.4	2	6935	5	67894	
13	OCH288	Moana	<LOD	12	<LOD	6	554	4	<LOD	2	<LOD	1	1444	5	14622	
14	OCH276-C	Moana	1229	19	848	10	1964	8	1031	4	524	3	26945	13	329089	
15	OCH254-A	Moana	3214	19	<LOD	8	860	6	459	3	174	2	15159	10	165377	
16	OCH142-B	Moana	1031	17	494	9	2169	7	293	3	148	2	11048	8	120230	
17	OCH019	Moana	<LOD	11	<LOD	6	129	4	<LOD	2	<LOD	1	2400	4	22190	
18	OCH036-A	Moana	<LOD	10	4	7	665	5	<LOD	2	<LOD	1	491	3	5879	
19	OCH275-C	Moana	228	9	<LOD	4	54.2	2	0.8	1	53.9	0.9	982	3	35503	
20	OCH275-D	Moana	596	9	<LOD	4	386	3	119	2	163	1	2118	4	63331	
21	OCH254-B	Moana	<LOD	6	<LOD	2	<LOD	1	<LOD	0.9	<LOD	0.6	81.7	1	6242	
22	OCH020-D	Moana	<LOD	7	<LOD	4	1066	4	<LOD	1	<LOD	0.7	153	2	8949	
23	OCH036-C	Moana	<LOD	6	<LOD	4	759	3	<LOD	1	<LOD	0.6	<LOD	1	3461	
24	OCH037-C	Moana	371	8	<LOD	4	394	3	<LOD	1	50.2	0.9	853	3	32171	
25	OCH036-B	Moana	<LOD	5	<LOD	2	<LOD	2	<LOD	0.8	<LOD	0.5	<LOD	0.9	827	
26	OCH294	Moana	<LOD	6	<LOD	2	<LOD	1	<LOD	0.8	<LOD	0.6	<LOD	1	2928	
27	OCH020-C	Moana (sample 2)	<LOD	11	<LOD	5	841	4	<LOD	1	<LOD	0.8	418	2	5849	
28	OCH101-C	Moana N-6	<LOD	12	<LOD	12	302	4	<LOD	2	<LOD	1	2063	4	20309	
29	OCH050	Pukatoo	9315	35	4	9	1703	5	1373	3	374	2	22758	8	251427	
30	OCH024-A	Pukatoo	<LOD	17	<LOD	8	910	6	<LOD	4	9.8	3	6152	10	60005	
31	OCH024-B	Pukatoo	618	10	45	5	467	4	646	2	321	2	3690	5	120830	
32	OCH050-A	Pukatoo	<LOD	7	<LOD	3	<LOD	2	<LOD	1	3.3	0.8	456	2	18219	
33	OCH067	Wilgie Mia	30552	34	<LOD	9	1011	5	76.4	3	215	2	5909	6	135746	
34																
35																
36																
37																
38																
39																
40																
41																
42																
43																
44																
45																
46																
47																

1														
2														
3														
4	OCH260	Wilgie Mia	4157	16	<LOD	4	<LOD	3	<LOD	1	<LOD	1	880	3 23843
5	OCH063	Wilgie Mia	52403	44	<LOD	11	1448	6	202	3	375	2	8838	8 210901
6	OCH117-A	Wilgie Mia	30397	33	<LOD	9	1021	5	46.8	3	131	2	12120	8 183097
7	OCH118-A	Wilgie Mia	38576	37	<LOD	10	1547	6	234	3	261	2	14918	9 233004
8	OCH258-A	Wilgie Mia	4258	17	<LOD	6	1048	4	<LOD	2	<LOD	1	1919	3 26701
9	OCH277	Wilgie Mia	27329	33	<LOD	8	803	5	97.7	3	213	2	5945	7 129713
10	OCH257	Wilgie Mia	20611	30	<LOD	7	566	4	17	2	139	2	4424	6 97080
11	OCH061	Wilgie Mia	<LOD	17	<LOD	5	50	3	72.3	2	19.4	1	6935	4 67894
12	OCH064-A	Wilgie Mia	<LOD	22	263	6	810	3	529	2	213	1	17044	5 175920
13	OCH264-A	Wilgie Mia	<LOD	13	<LOD	5	566	3	<LOD	1	<LOD	0.9	2688	2 25931
14	OCH065-A	Wilgie Mia	<LOD	12	<LOD	6	453	5	214	2	88	1	9979	3 99019
15	OCH117-E	Wilgie Mia	<LOD	8	<LOD	4	620	3	1.8	1	64.5	1	947	3 35025
16	OCH117-Y	Wilgie Mia	2708	14	675	7	1360	6	983	3	913	2	9350	8 330997
17	OCH277-A	Wilgie Mia	<LOD	5	<LOD	2	<LOD	1	<LOD	0.8	<LOD	0.6	<LOD	1 2816
18	OCH065-B	Wilgie Mia	243	9	<LOD	4	711	3	<LOD	1	11.8	0.8	404	2 17692
19	OCH260-A	Wilgie Mia	174	9	<LOD	4	309	3	218	2	234	1	2516	4 86304
20	OCH264-C	Wilgie Mia	<LOD	7	<LOD	3	293	3	<LOD	1	7.5	0.8	402	2 17422
21	OCH119	Wilgie Mia N-2b	3732	21	1330	12	2460	9	1525	5	853	4	34757	15 449933
22														
23														
24														
25														
26														
27														
28														
29														
30														
31														
32														
33														
34														
35														
36														
37														
38														
39														
40														
41														
42														
43														
44														
45														
46														
47														

	Fe LOD	Cu	Cu LOD	Zn	Zn LOD	As	As LOD	Rb	Rb LOD	Sr	Sr LOD	PbL	Pb LOD
1													
2													
3													
4													
5	10	<LOD	1	<LOD	1	5.8	0.7	<LOD	0.3	18.6	0.4	<LOD	0.8
6	13	<LOD	2	<LOD	1	<LOD	0.9	<LOD	0.3	<LOD	0.4	71	1
7	8	<LOD	2	60.8	1	<LOD	0.9	26.8	0.4	36.6	0.5	385	1
8	14	<LOD	2	<LOD	2	<LOD	0.9	25.2	0.4	16.9	0.5	233	1
9	10	<LOD	2	<LOD	1	<LOD	0.8	22.9	0.4	30.2	0.5	31.6	1
10	14	<LOD	2	<LOD	1	<LOD	0.8	66.3	0.4	39.7	0.6	44.5	1
11	11	<LOD	0.9	<LOD	0.7	<LOD	0.5	0.87	0.2	<LOD	0.3	59.8	0.7
12	14	<LOD	2	738	3	<LOD	1	11.3	0.5	240	0.7	418	2
13	11	<LOD	1	436	2	35.4	0.6	<LOD	0.2	54.7	0.3	54.9	0.7
14	10	<LOD	1	189	1	<LOD	0.5	<LOD	0.2	41.2	0.3	27.7	0.7
15	12	<LOD	1	<LOD	1	<LOD	0.7	132	0.5	290	0.6	22.7	0.9
16	9	<LOD	0.9	<LOD	0.7	<LOD	0.5	13.3	0.3	14	0.3	12.5	0.6
17	4	<LOD	0.9	<LOD	0.7	<LOD	0.4	9.49	0.2	13.7	0.3	<LOD	0.6
18	11	<LOD	1	<LOD	0.7	<LOD	0.6	17.6	0.3	<LOD	0.3	212	0.9
19	4	<LOD	0.9	<LOD	0.7	<LOD	0.4	3.96	0.2	16.9	0.3	<LOD	0.6
20	6	<LOD	0.9	<LOD	0.7	<LOD	0.4	35.6	0.3	73.3	0.4	5.8	0.6
21	14	<LOD	2	<LOD	1	<LOD	0.9	30.3	0.5	34	0.6	75.8	1
22	7	<LOD	1	<LOD	0.9	<LOD	0.6	121	0.4	297	0.5	75.2	0.8
23	9	<LOD	2	<LOD	1	<LOD	0.8	25.4	0.5	65.7	0.5	41.2	1
24	14	<LOD	2	<LOD	1	24.1	0.8	26.2	0.4	30	0.5	21.8	1
25	14	<LOD	2	<LOD	1	<LOD	0.9	61.4	0.4	20.9	0.5	74.2	1
26	14	<LOD	2	<LOD	1	<LOD	0.9	75.1	0.4	45.2	0.5	64.5	1
27	12	<LOD	2	<LOD	1	<LOD	0.8	212	0.6	368	0.8	81.6	1
28	13	<LOD	2	<LOD	1	<LOD	0.8	<LOD	0.3	<LOD	0.3	58.6	1
29	13	<LOD	2	<LOD	2	<LOD	0.9	<LOD	0.3	<LOD	0.3	96.8	1
30	10	<LOD	1	<LOD	1	<LOD	0.6	15.5	0.3	<LOD	0.3	<LOD	0.8
31	8	<LOD	2	<LOD	1	<LOD	0.5	<LOD	0.3	<LOD	0.3	<LOD	0.7
32	12	<LOD	1	<LOD	1	<LOD	0.6	10	0.3	<LOD	0.3	<LOD	0.8
33	5	<LOD	1	<LOD	1	<LOD	0.6	47	0.4	6.7	0.4	<LOD	0.8
34													
35													
36													
37													
38													
39													
40													
41													
42													
43													
44													
45													
46													
47													

1													
2													
3													
4	8	<LOD	1	<LOD	0.9	<LOD	0.6	<LOD	0.3	<LOD	0.3	<LOD	0.8
5	13	<LOD	2	<LOD	1	<LOD	0.9	<LOD	0.3	<LOD	0.3	107	1
6	12	<LOD	2	<LOD	1	<LOD	0.9	<LOD	0.3	<LOD	0.3	94.2	1
7	12	<LOD	2	<LOD	1	<LOD	1	<LOD	0.3	<LOD	0.4	173	1
8	9	<LOD	1	<LOD	1	<LOD	0.6	<LOD	0.3	<LOD	0.3	<LOD	0.7
9	13	<LOD	2	<LOD	1	<LOD	0.8	<LOD	0.3	<LOD	0.3	44.3	1
10	13	<LOD	2	<LOD	1	<LOD	0.7	<LOD	0.3	<LOD	0.3	16.3	1
11	13	<LOD	2	<LOD	1	<LOD	0.7	<LOD	0.3	<LOD	0.3	16.3	1
12	10	<LOD	1	<LOD	1	<LOD	0.6	19.9	0.3	21.9	0.3	74.9	0.8
13	13	<LOD	1	<LOD	1	<LOD	0.6	25.2	0.3	16.9	0.3	233	0.9
14	13	<LOD	1	<LOD	1	<LOD	0.6	25.2	0.3	16.9	0.3	233	0.9
15	6	<LOD	1	<LOD	0.9	<LOD	0.6	22.9	0.3	30.2	0.3	31.6	0.7
16	9	<LOD	2	<LOD	1	19.7	0.8	25.4	0.4	27	0.5	72.9	1
17	9	<LOD	1	<LOD	0.8	3	0.5	<LOD	0.2	<LOD	0.3	<LOD	0.6
18	9	<LOD	1	<LOD	0.8	3	0.5	<LOD	0.2	<LOD	0.3	<LOD	0.6
19	11	<LOD	1	<LOD	0.7	<LOD	0.8	40	0.3	<LOD	0.2	669	1
20	3	<LOD	0.9	<LOD	0.7	<LOD	0.4	<LOD	0.2	<LOD	0.3	<LOD	0.6
21	3	<LOD	0.9	<LOD	0.7	<LOD	0.4	<LOD	0.2	<LOD	0.3	<LOD	0.6
22	6	<LOD	1	<LOD	0.7	<LOD	0.4	<LOD	0.2	<LOD	0.3	<LOD	0.6
23	11	<LOD	1	<LOD	0.7	<LOD	0.5	1.2	0.2	<LOD	0.2	52.7	0.7
24	6	<LOD	1	<LOD	0.7	<LOD	0.4	1.35	0.2	<LOD	0.3	<LOD	0.6
25	6	<LOD	1	<LOD	0.7	<LOD	0.4	1.35	0.2	<LOD	0.3	<LOD	0.6
26	14	<LOD	2	<LOD	1	<LOD	1	60.5	0.5	<LOD	0.4	886	2
27													
28													
29													
30													
31													
32													
33													
34													
35													
36													
37													
38													
39													
40													
41													
42													
43													
44													
45													
46													
47													